On the Cause of Solar Differential Rotation
太陽差動自轉的成因

Ling-Hsiao Lyu

Institute of Space Science, National Central University

呂凌霄

中央大學太空科學研究所

11-years Solar Cycle Based on Sunspot Number

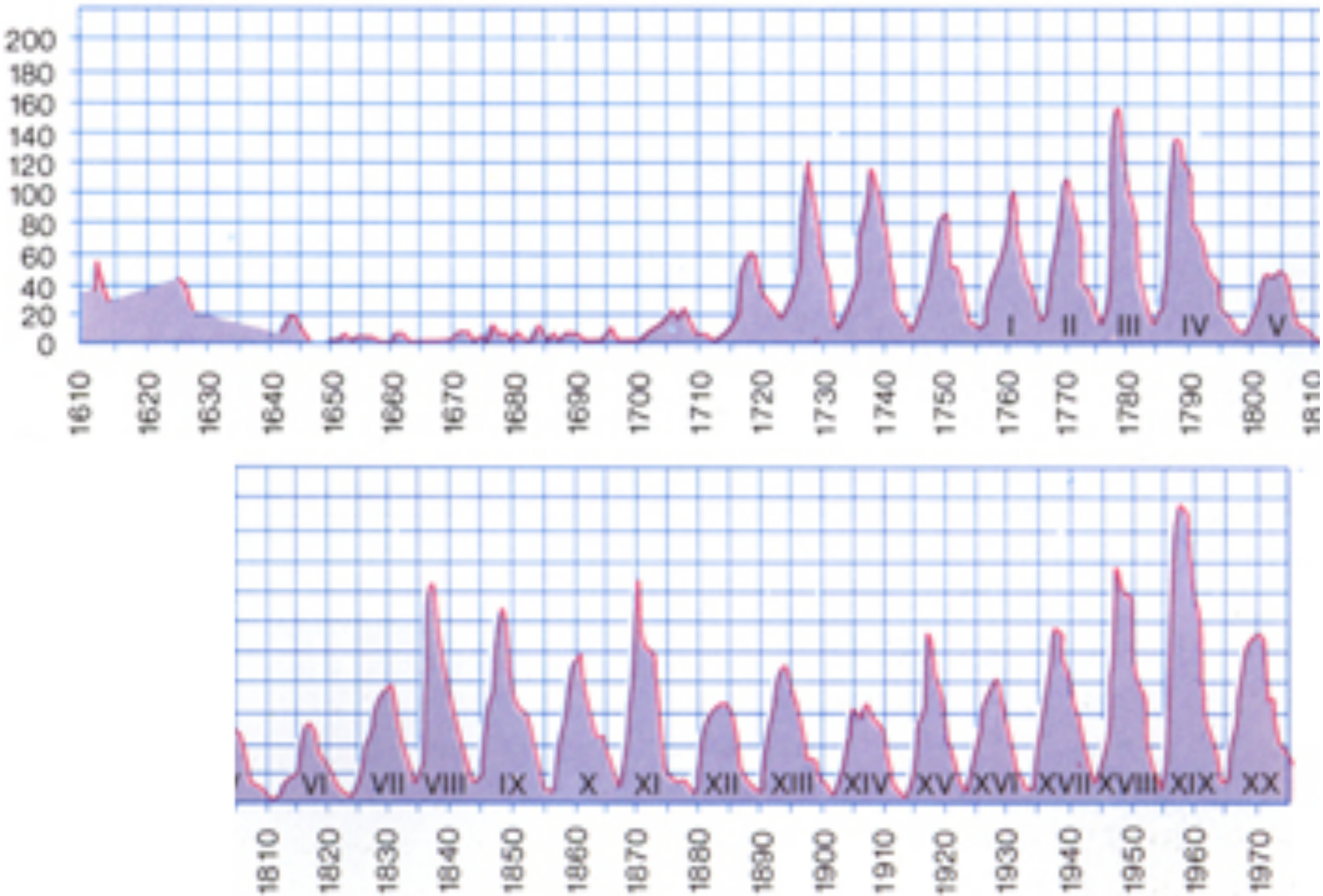

DAILY SUNSPOT AREA AVERAGED OVER INDIVIDUAL SOLAR ROTATIONS

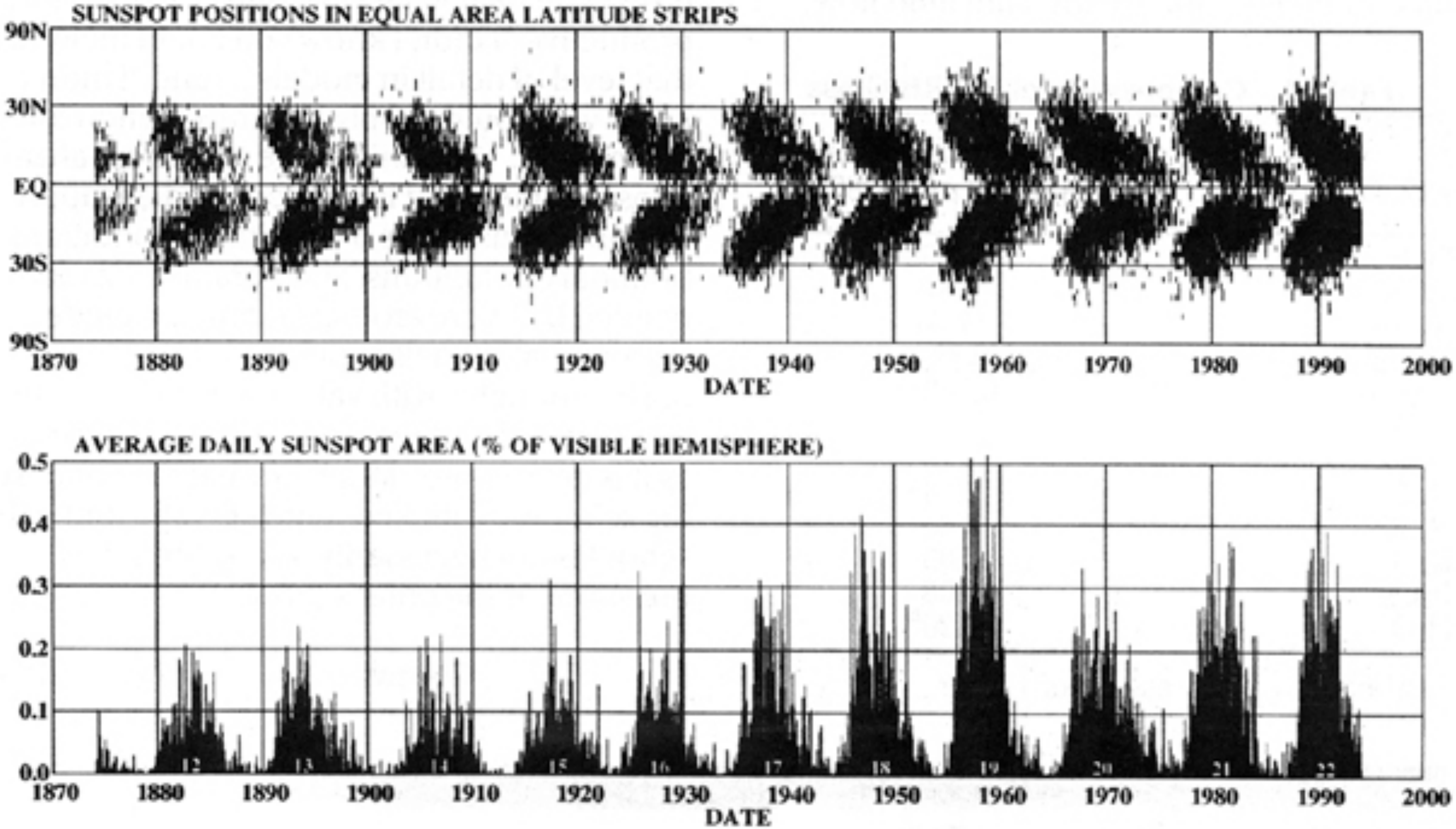

22-years Solar Cycle
Based on Leading Sunspot Magnetic Polarity

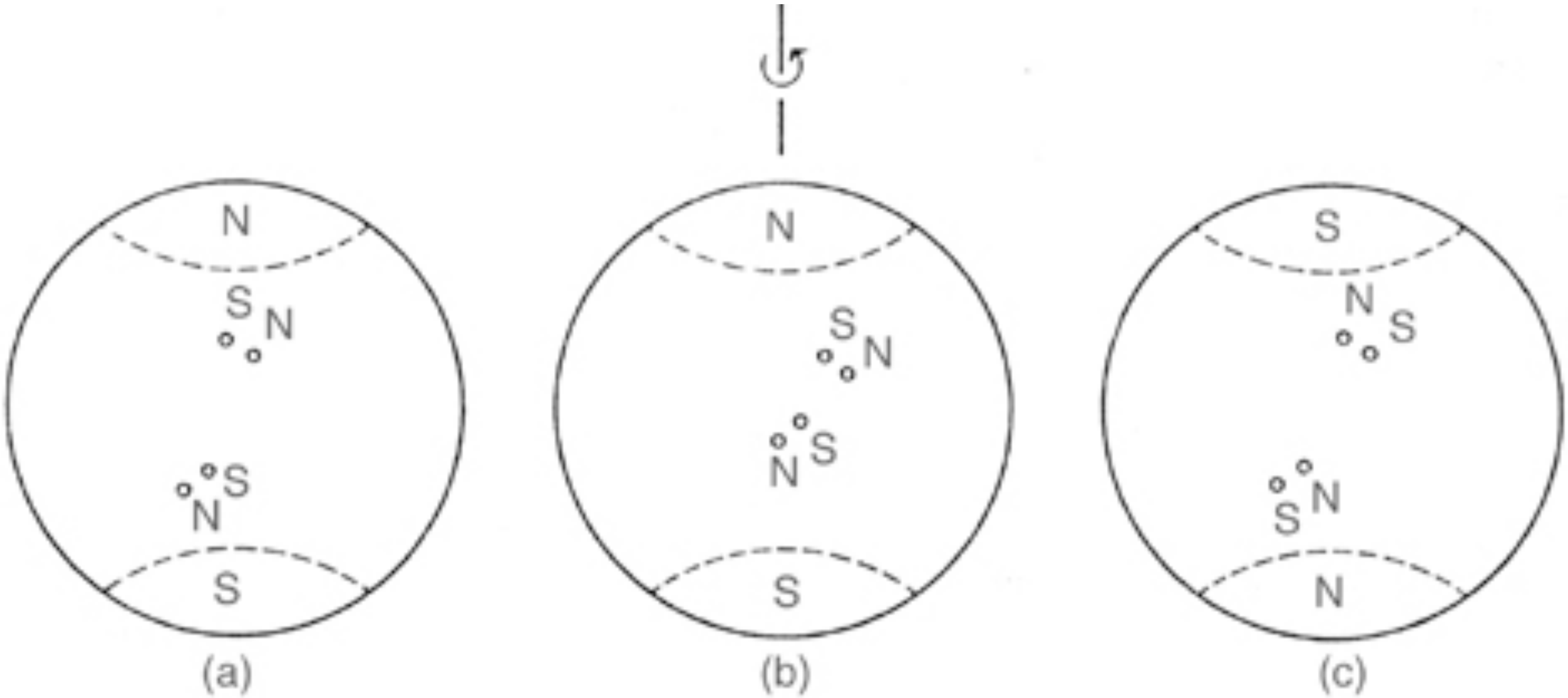

Solar Differential Rotation

--> Solar Dynamo (ww-effects, wa-effects)

-->22-years Magnetic Solar Cycle

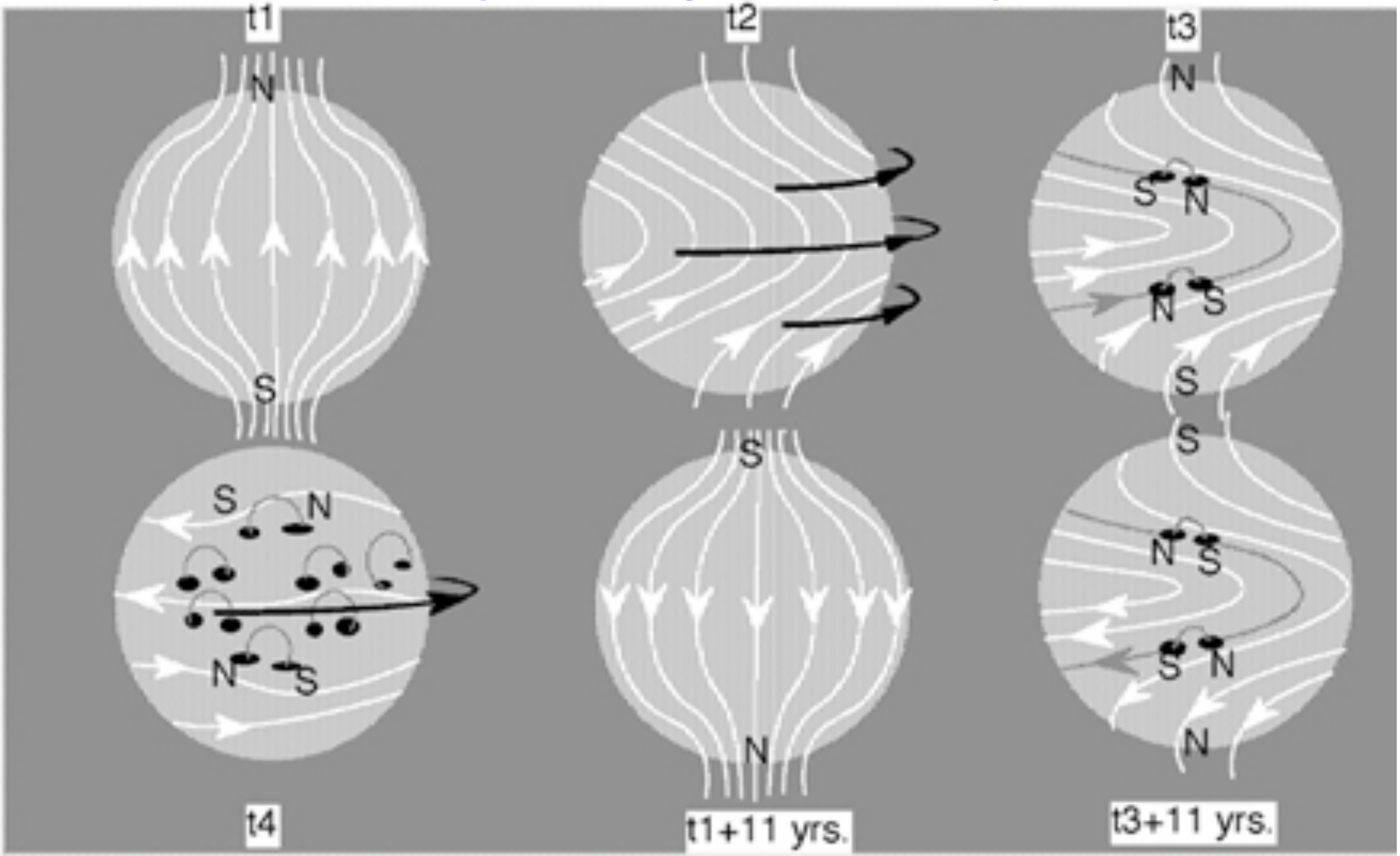

Differential rotation is the major cause of solar cycle!

What is the cause of solar differential rotation?

Differential Rotation in Solar Interior

SoHO/MDI Observation

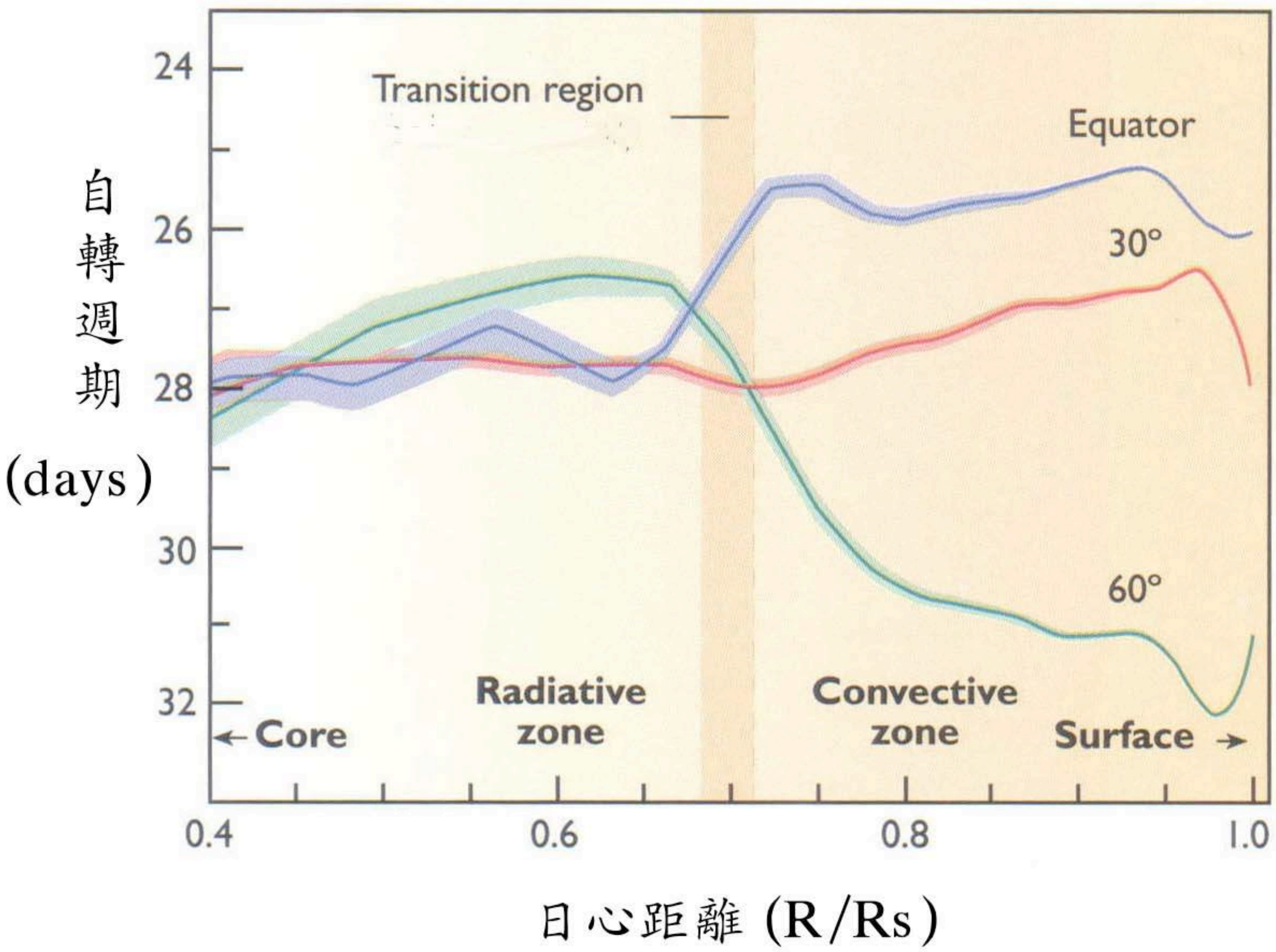

Solar Interior Structures

convection zone:
r=1~0.86Rs(old model)
r=1~0.7Rs(new model)

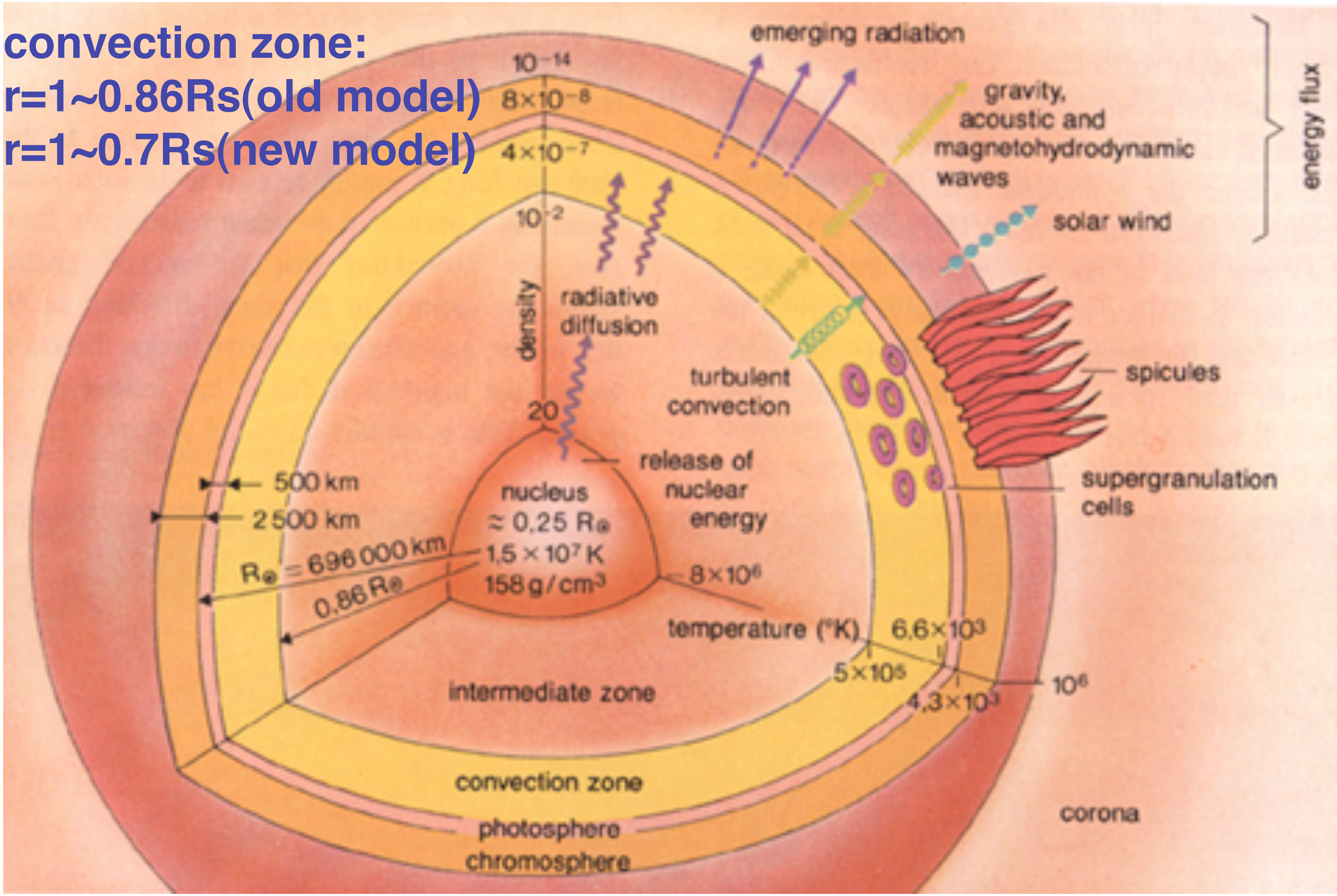

Sound Speed Distribution in Solar Interior

Abnormal plasma sound speed ($c^2=T/m$) distribution in the solar interior (MDI observation)

$\delta(c^2)>0$

$\delta(c^2)<0$

T : plasma temperature

m average mass

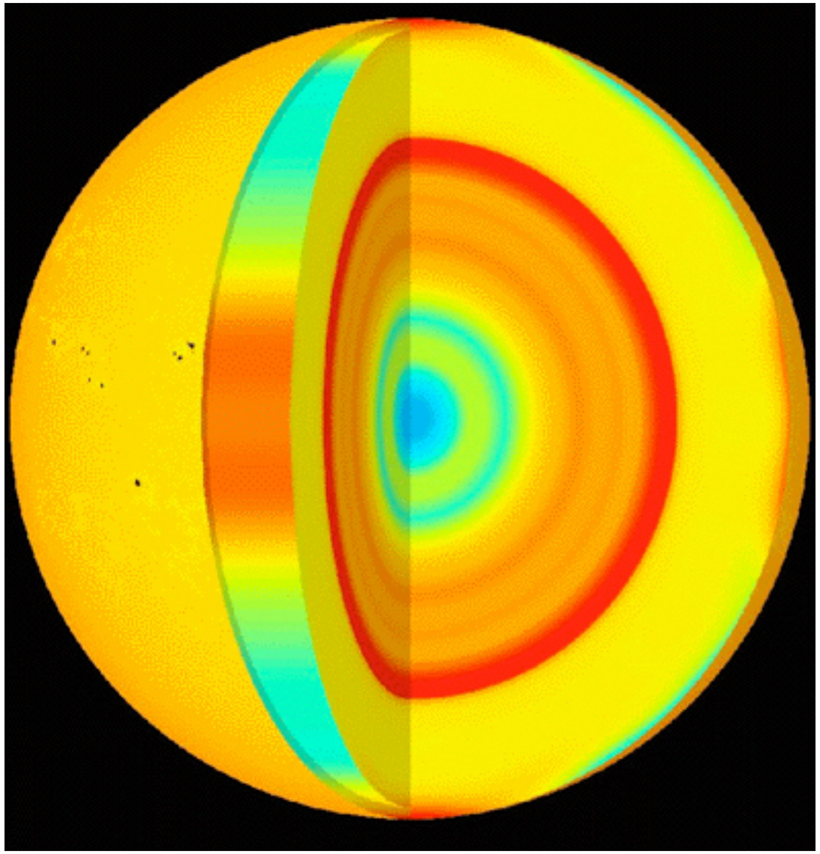

MDI Observations (Kosovichev et al., 1997)

(A) Differential Rotation

(B) Abnormal Plasma Temperature Distribution

Cause → Result

(A) → *Turbulence Heating* → (B)

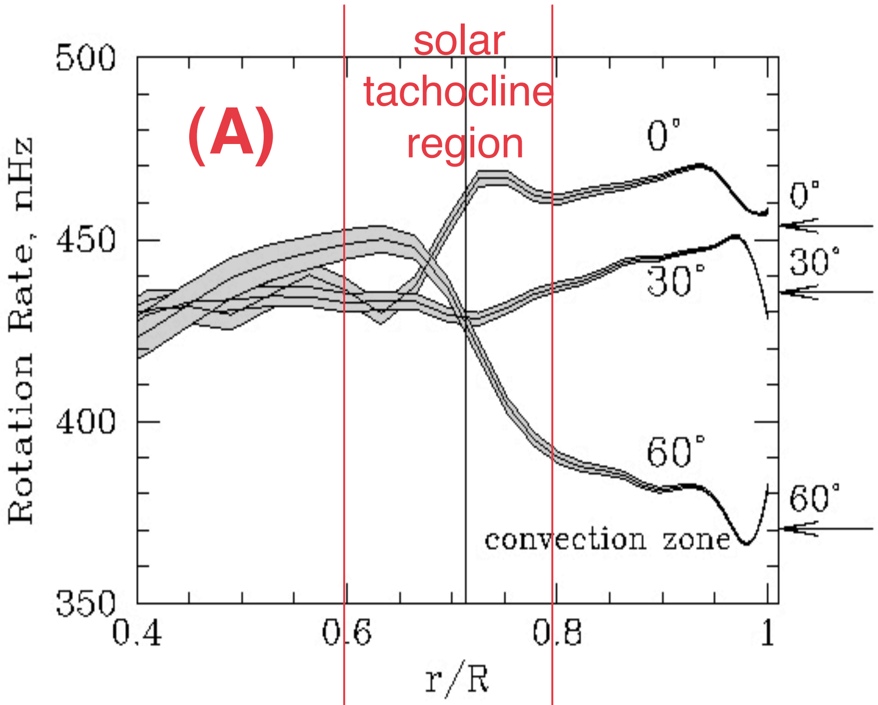

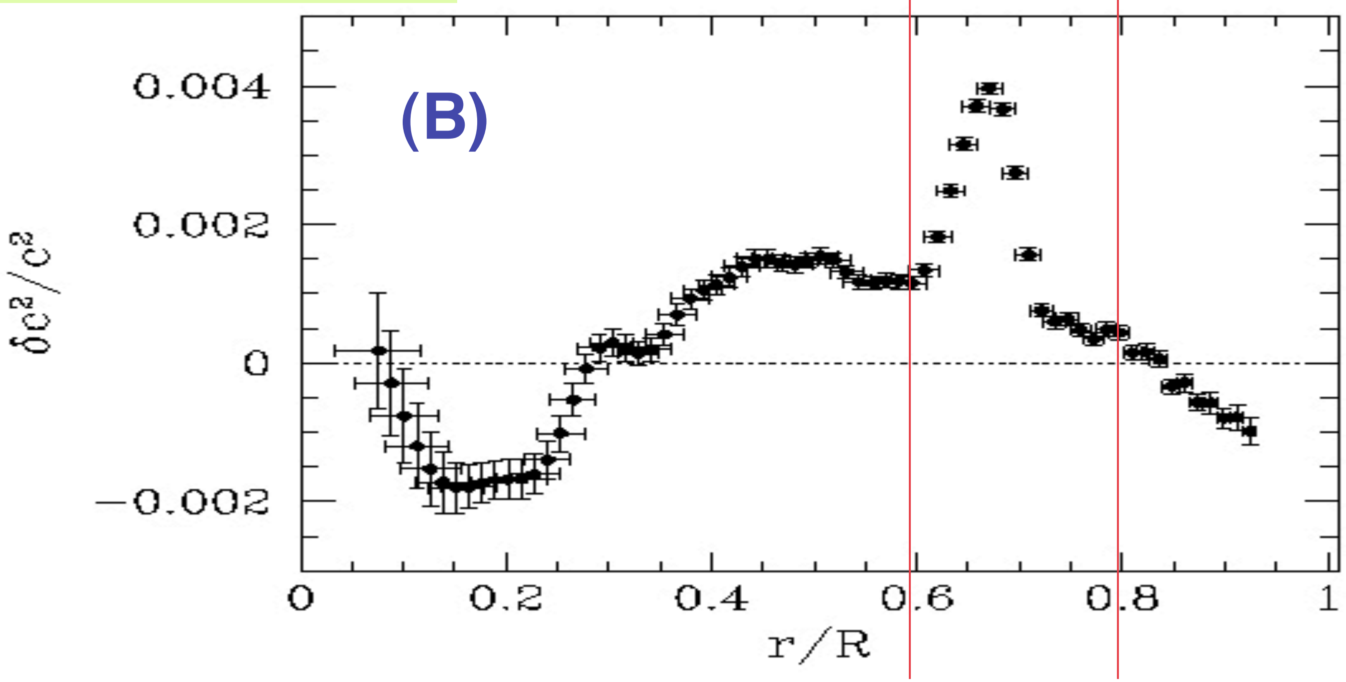

Averge Mass mDistribution in Standard Solar Model

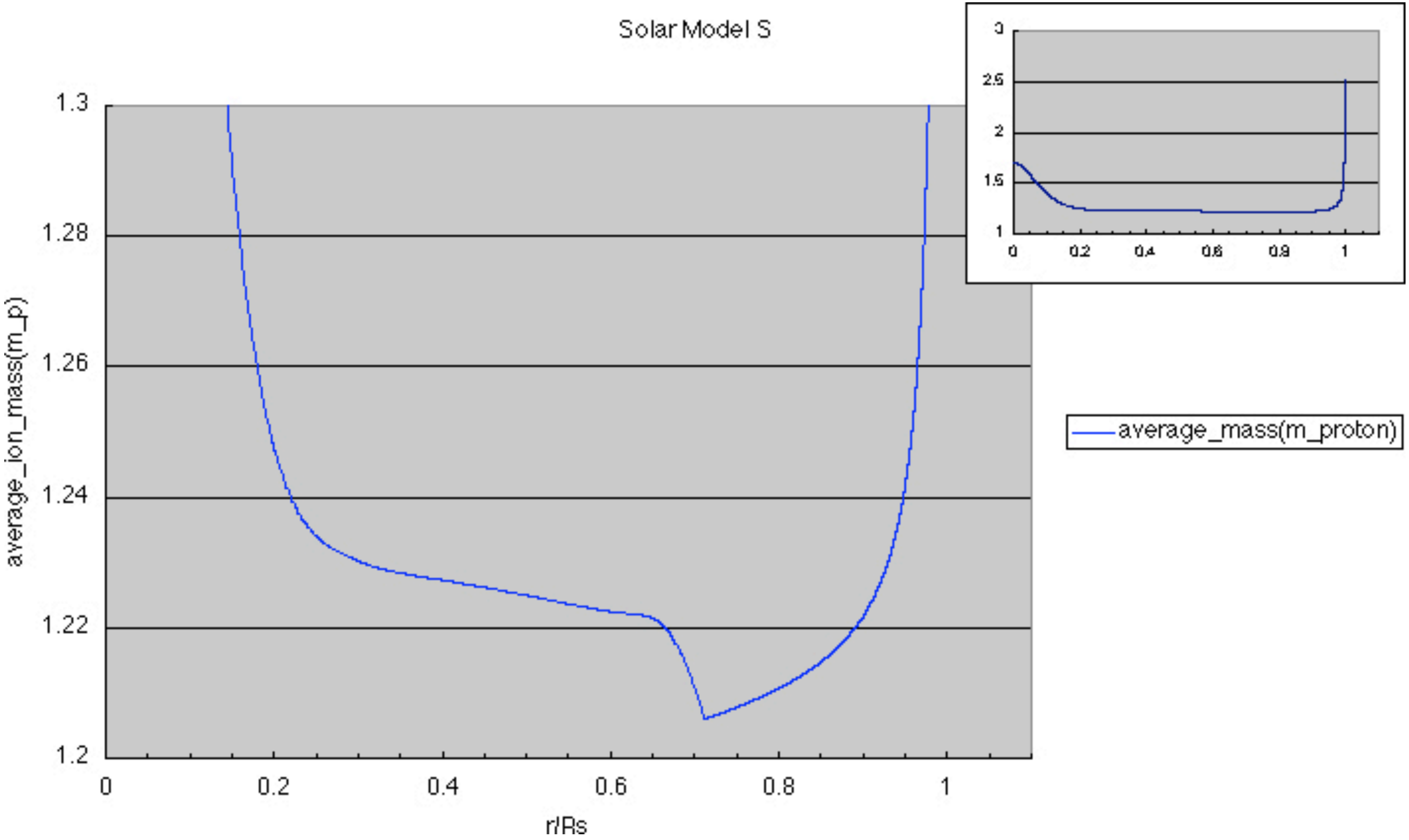

(C) Average Mass mDistribution in Standard Solar Model

Cause → Result

Under estimate mixing length
→Under estimate m
→Over estimate $c^2=T/m$
→ (B) Abnormal Plasma Temperature Distribution

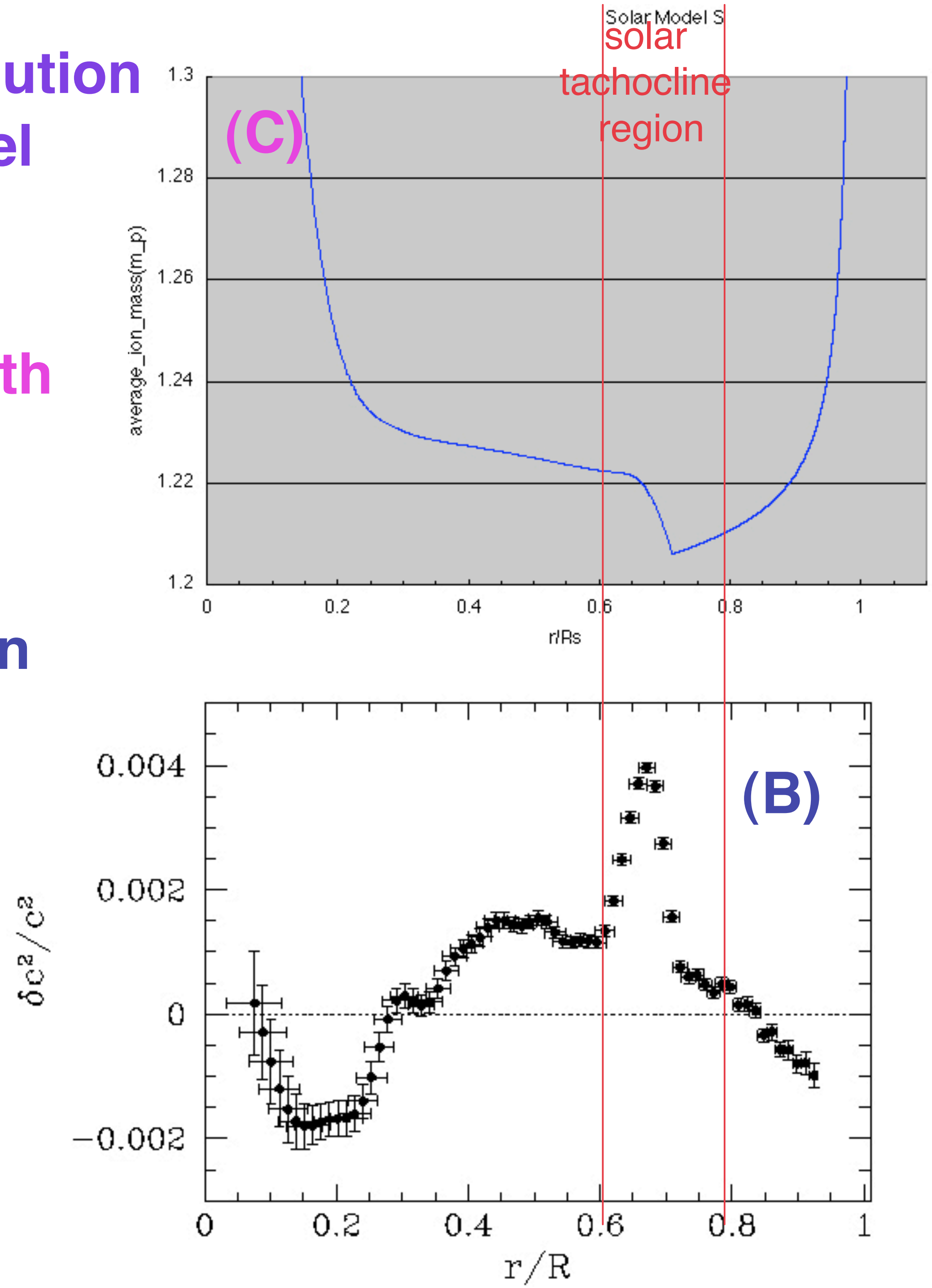

Sound Speed Distribution in Solar Interior

Abnormal plasma sound speed ($c^2=T/m$) distribution in the solar interior (MDI observation)

$\delta(c^2)>0$

$\delta(c^2)<0$

T : plasma temperature

m average mass

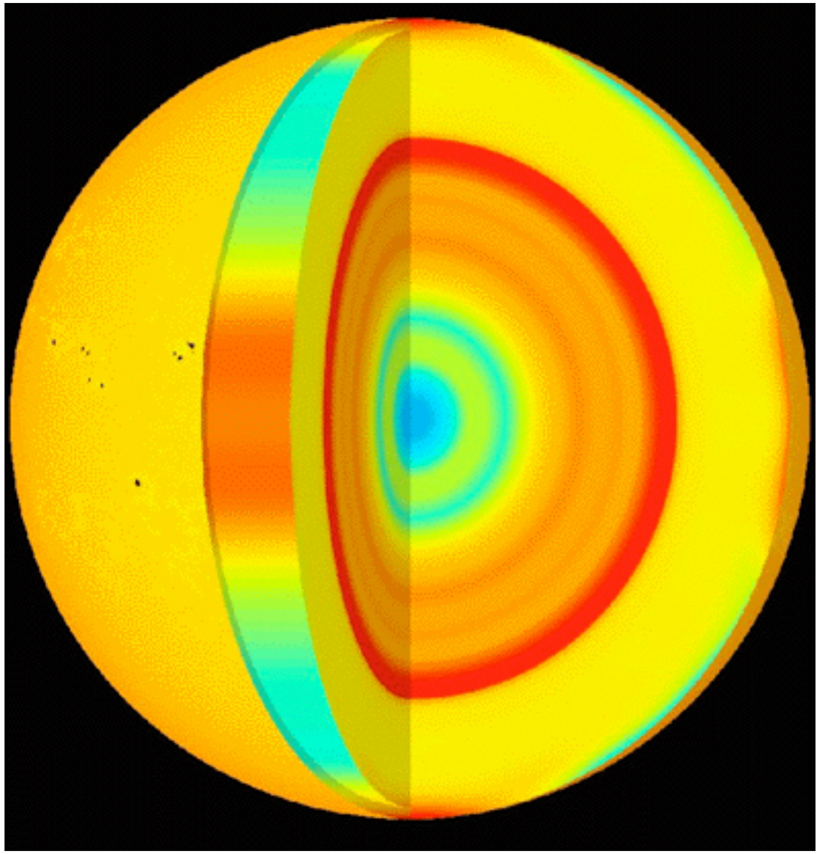

Our Explanation

We assume that a *normal* state means a hydrodynamic equilibrium state.

$$-\nabla p + \rho \mathbf{g} = 0 \quad \text{or} \quad -\frac{dp}{dr} = \rho g$$

Then, *abnormal* temperature profile in the solar tachocline region

indicates that $-\frac{dp}{dr} > \rho g$

To reach a steady state, there must be an *inward force* to make force balance in the r-direction.

We propose that

(1) abnormal temperature only occur in the middle and lower latitude region,

(2) the inward force is a $\mathbf{J} \times \mathbf{B}$ force , such that

$$\boxed{(-\frac{dp}{dr} - \rho g)\hat{r} + \mathbf{J} \times \mathbf{B} = 0} \quad \text{or} \quad \boxed{\mathbf{J} = (-\frac{dp}{dr} - \rho g)\hat{r} \times \frac{\mathbf{B}}{B^2}}$$

(3) absence of such inward force ($\mathbf{J} \times \mathbf{B}$) in the polar coronal hole region is because that $\boxed{\mathbf{B} = B_r \hat{r}}$ in the polar coronal hole region.

Our Explanation on Abnormal c^2 Distribution

Abnormal plasma sound speed ($c^2=T/m$) distribution in the solar interior (MDI observation)

$\delta(c^2)>0$

$\delta(c^2)<0$

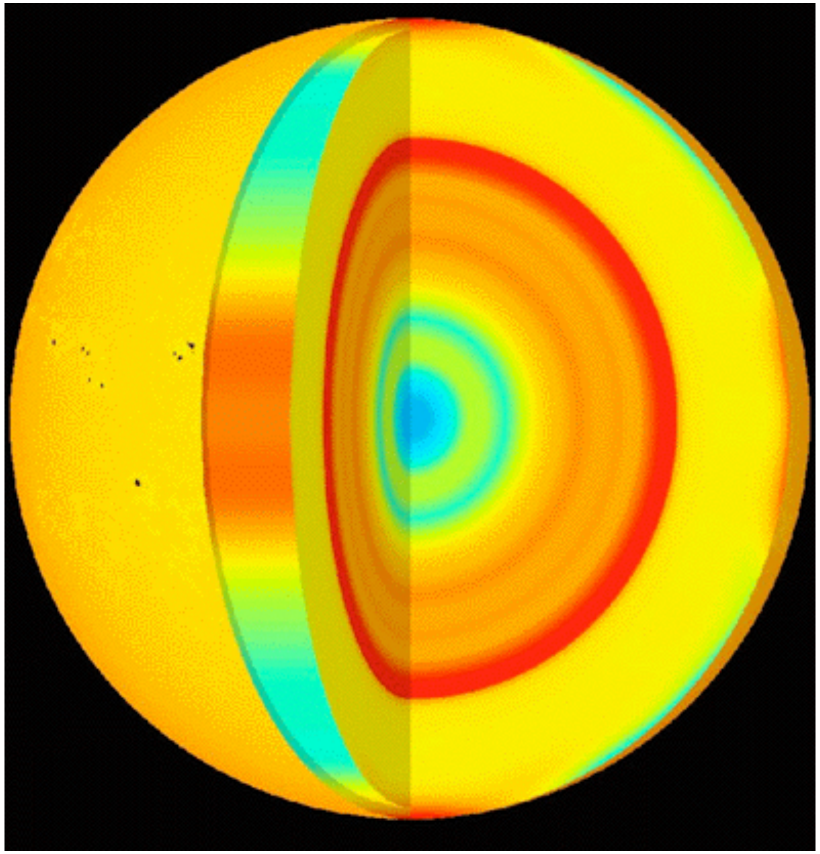

Plasma Temperature

$T_1 > T_2 > T_3$

Average Mass:

$m_1 > m_2 > m_3$

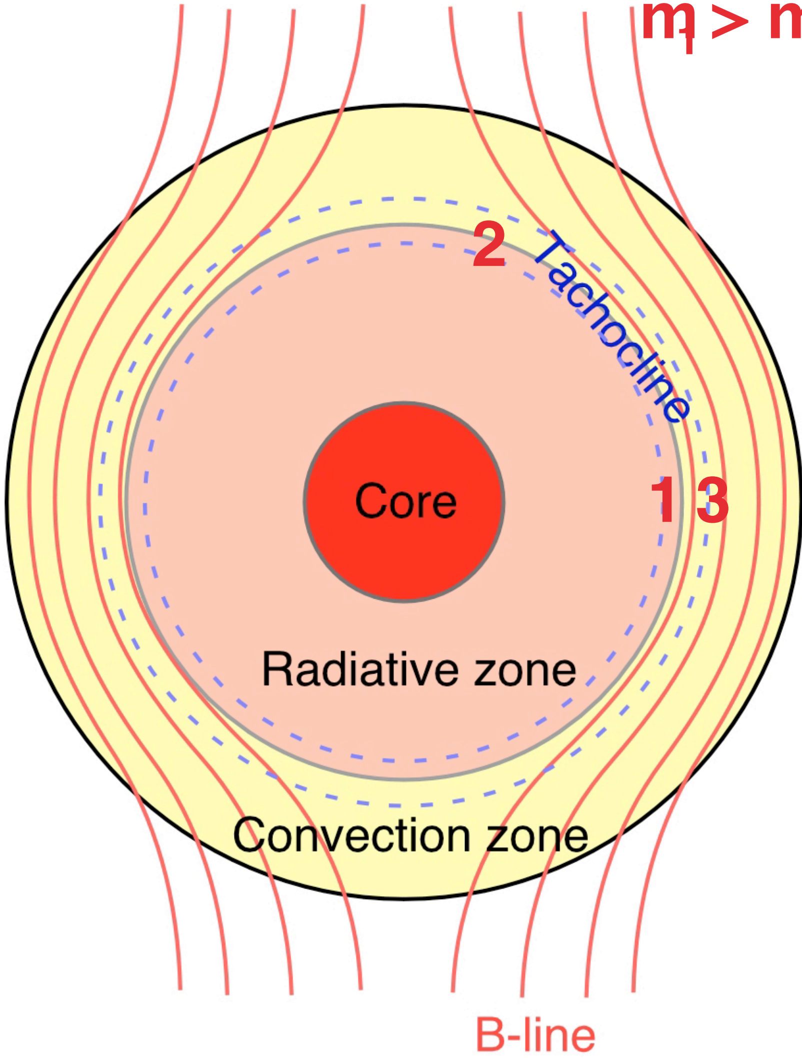

Evidence on
Smaller mixing length in the low latitude region
Large mixing length in the high latitude region

Average mass

$m_1 > m_2 > m_3$

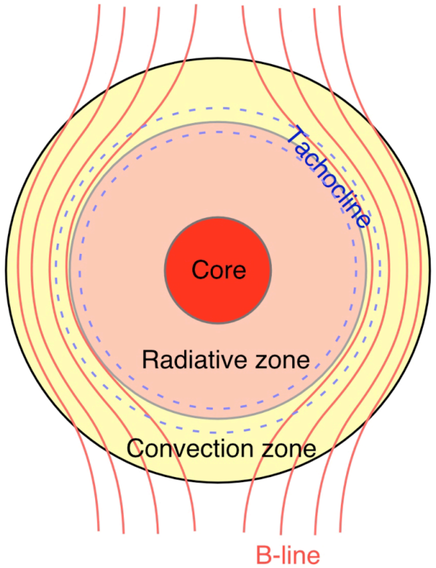

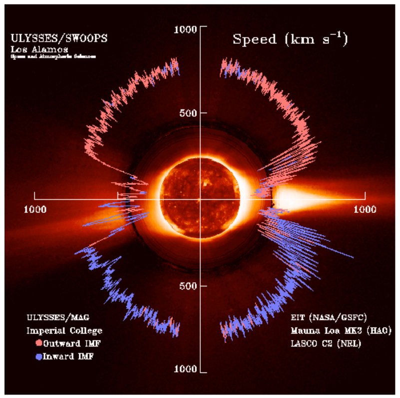

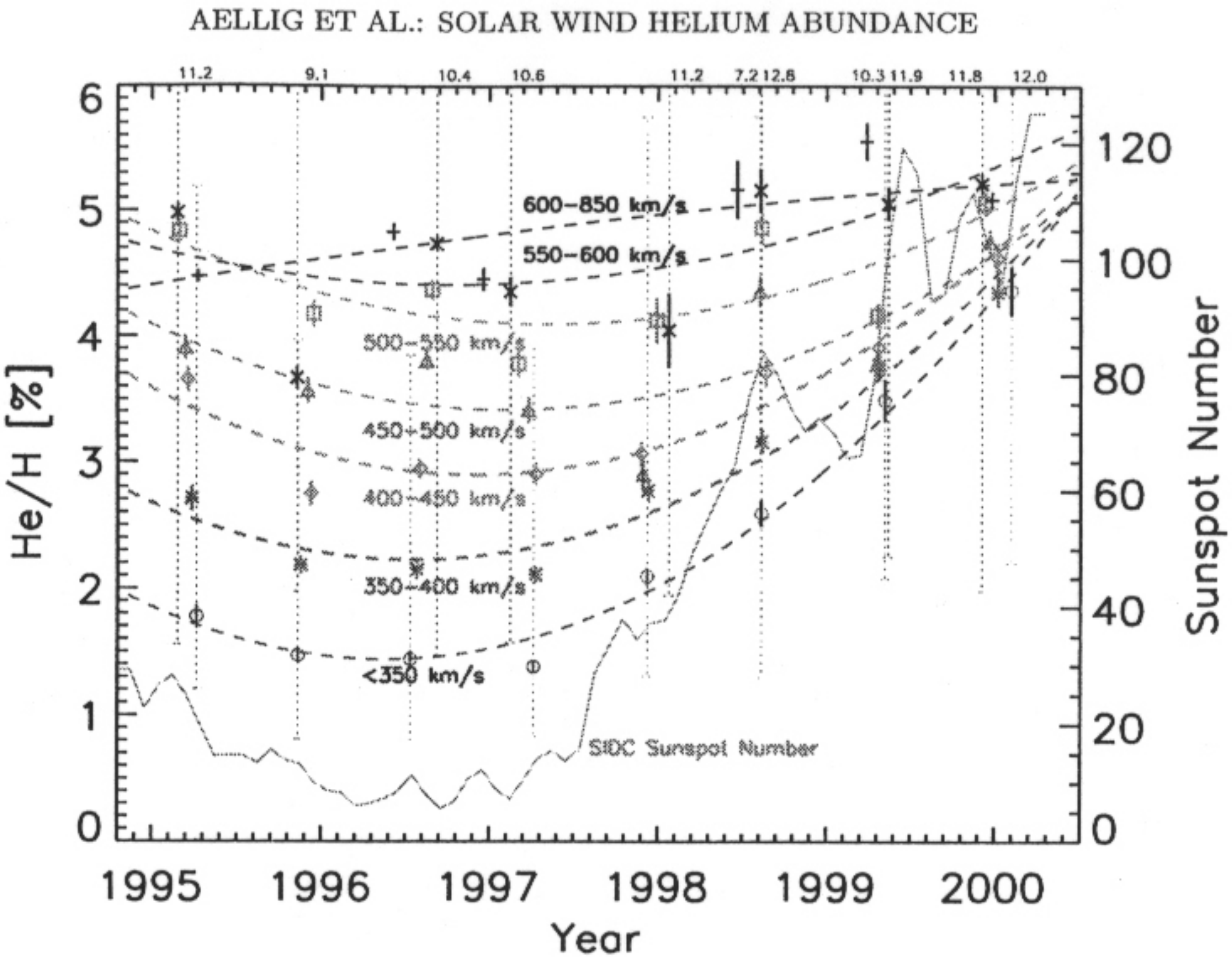

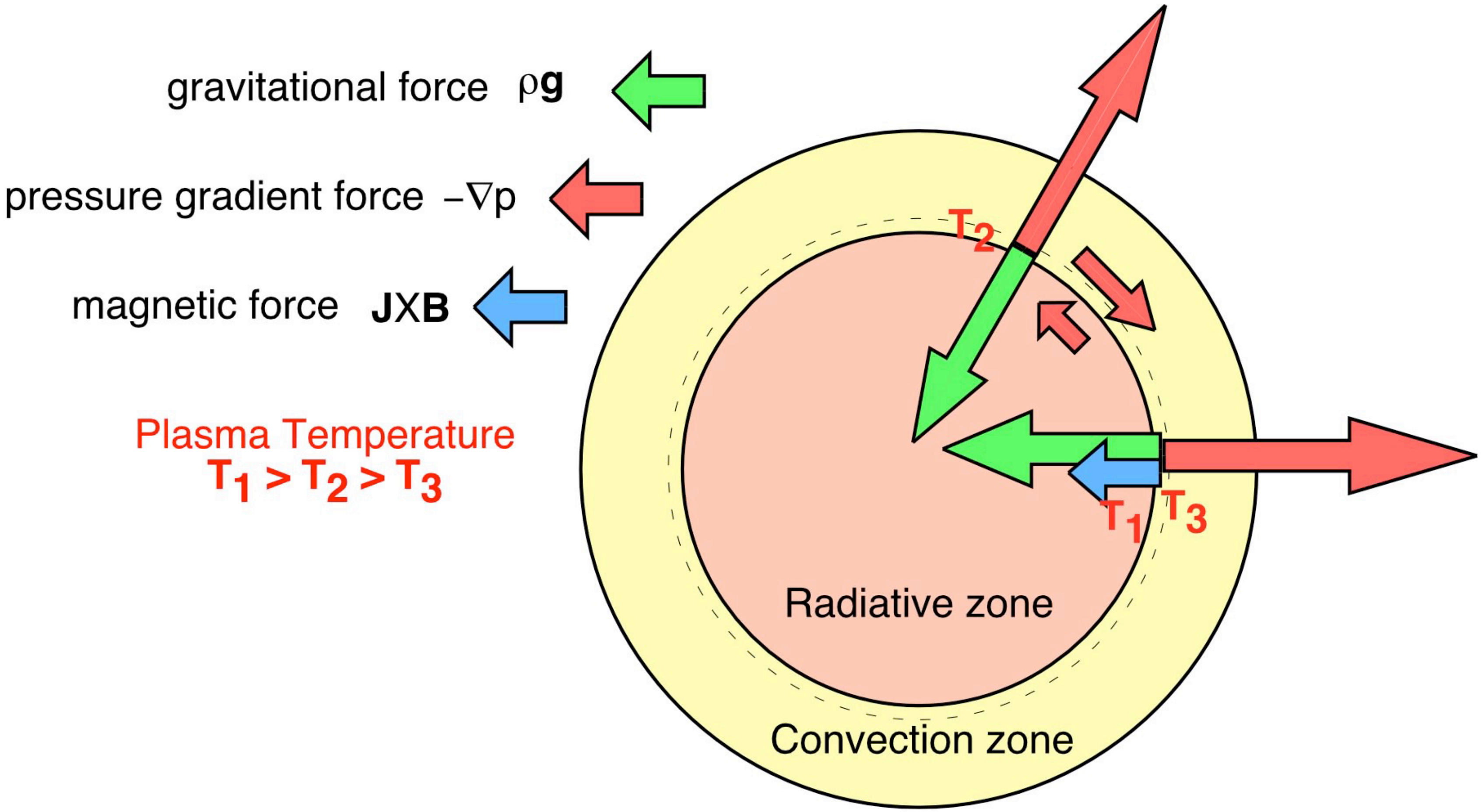

Zonal flow can lead to horizontal force balance in a rotational star or planet with latitudinal temperature gradient

Upper-half tachocline: (in solar convection zone)
Poleward temperature gradient →easterly wind
Lower-half tachocline: (in solar radiative zone)
Equatorward temperature gradient → westerly wind

Easterly wind in the upper-half solar tachocline region (in solar convection zone).

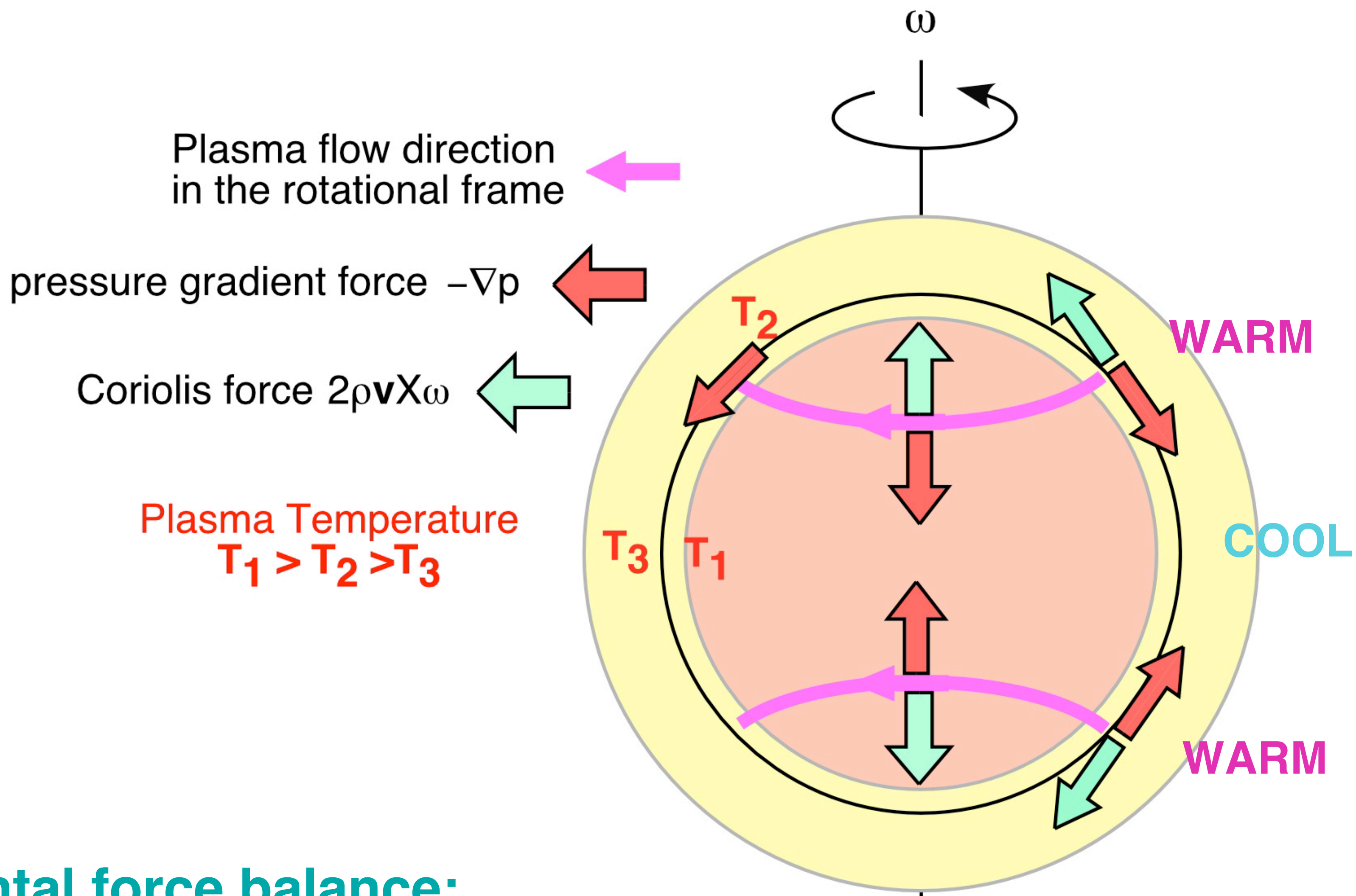

Horizontal force balance:

Poleward temperature gradient →easterly wind

Westerly wind in the lower-half solar tachocline region (in solar radiative zone)

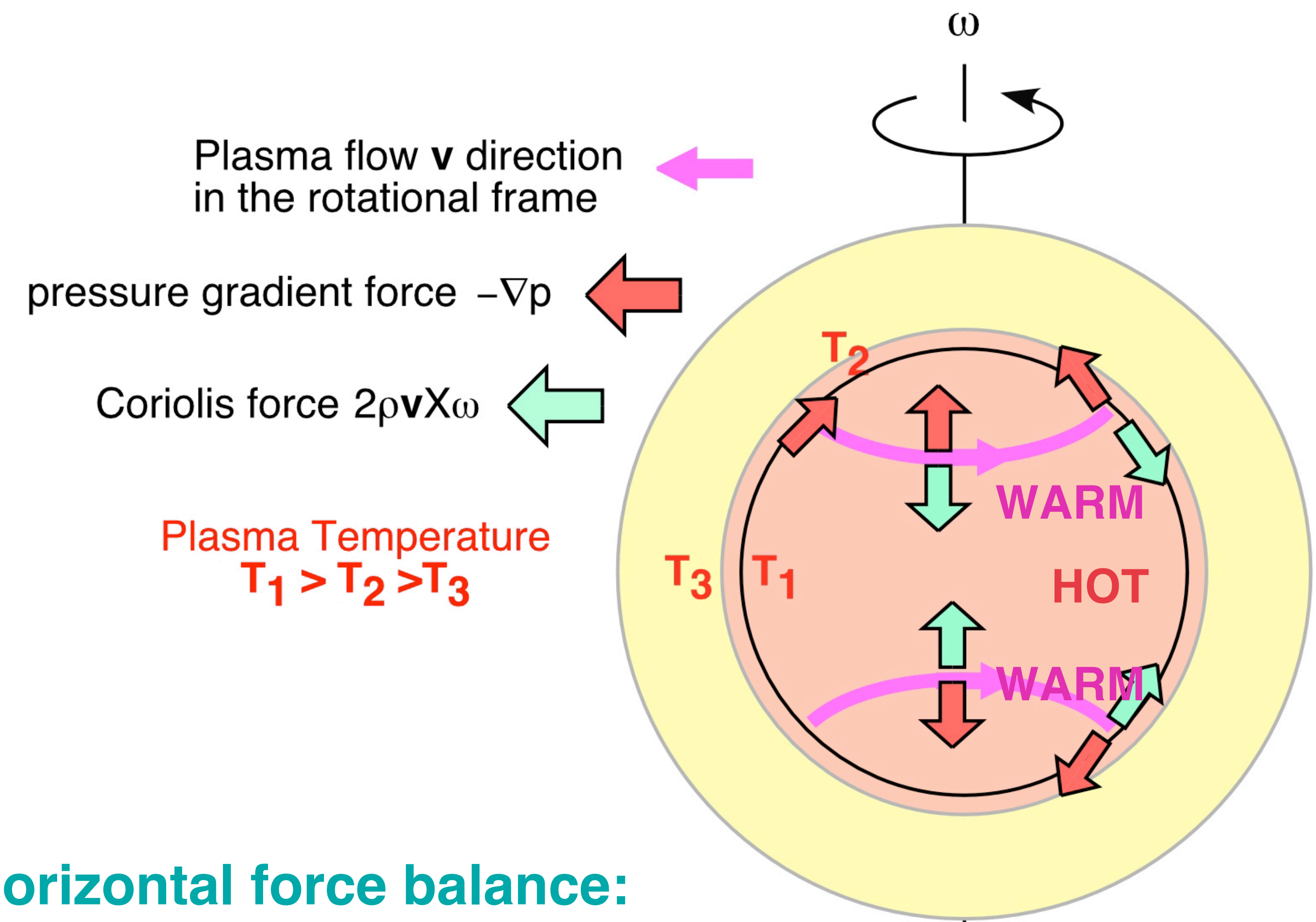

Horizontal force balance:

Equatorward temperature gradient → westerly wind

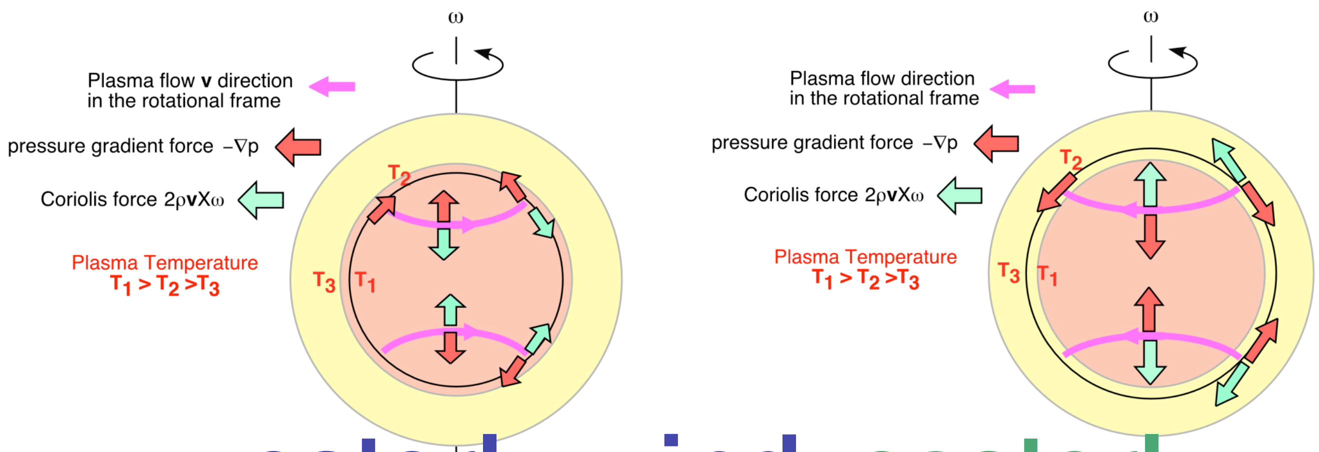

~60 degrees **westerly wind** **easterly wind**

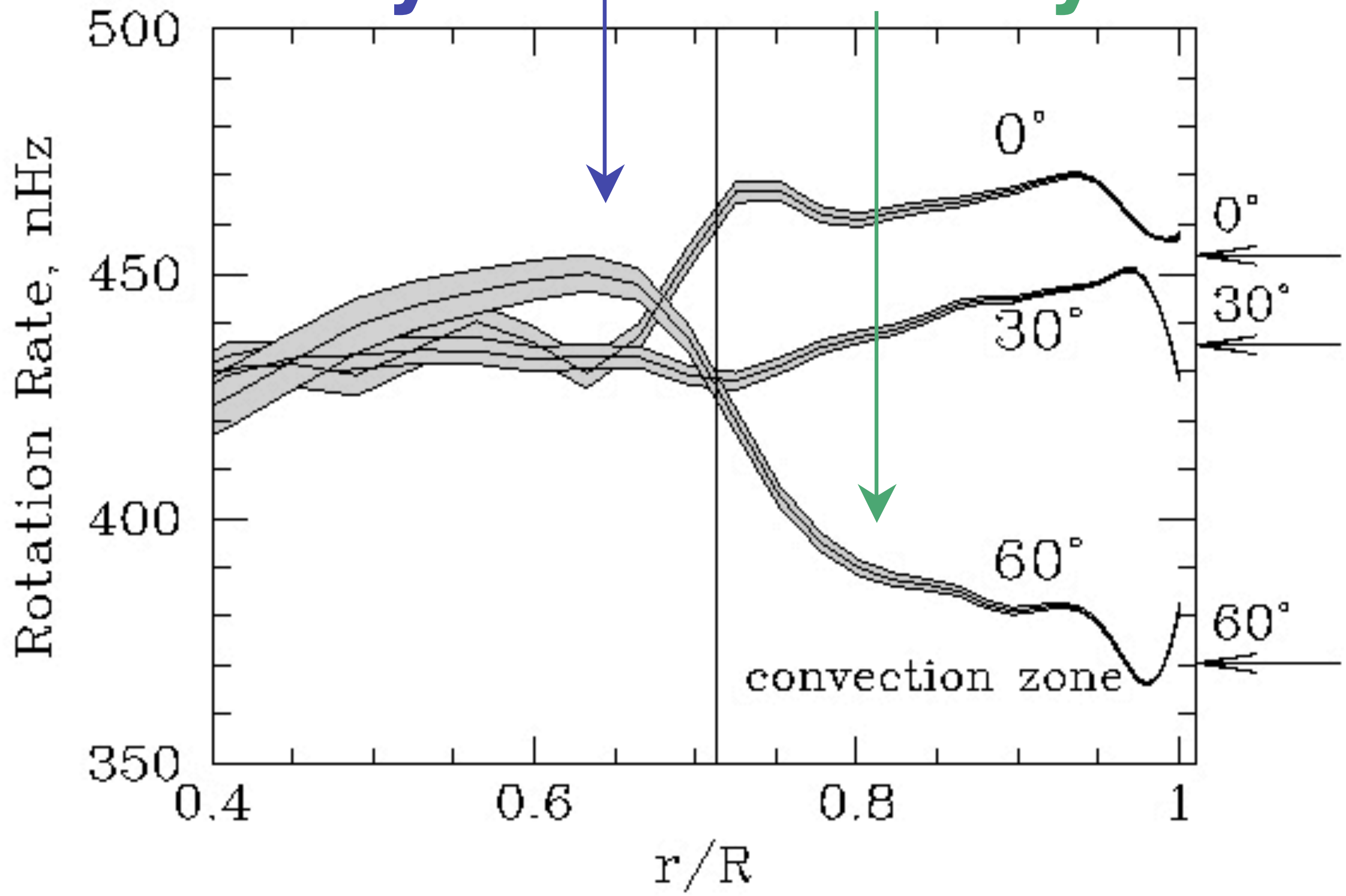

Initial formation of solar filaments' magnetic field

BBO Hα observation

of solar filaments 05/11/1998

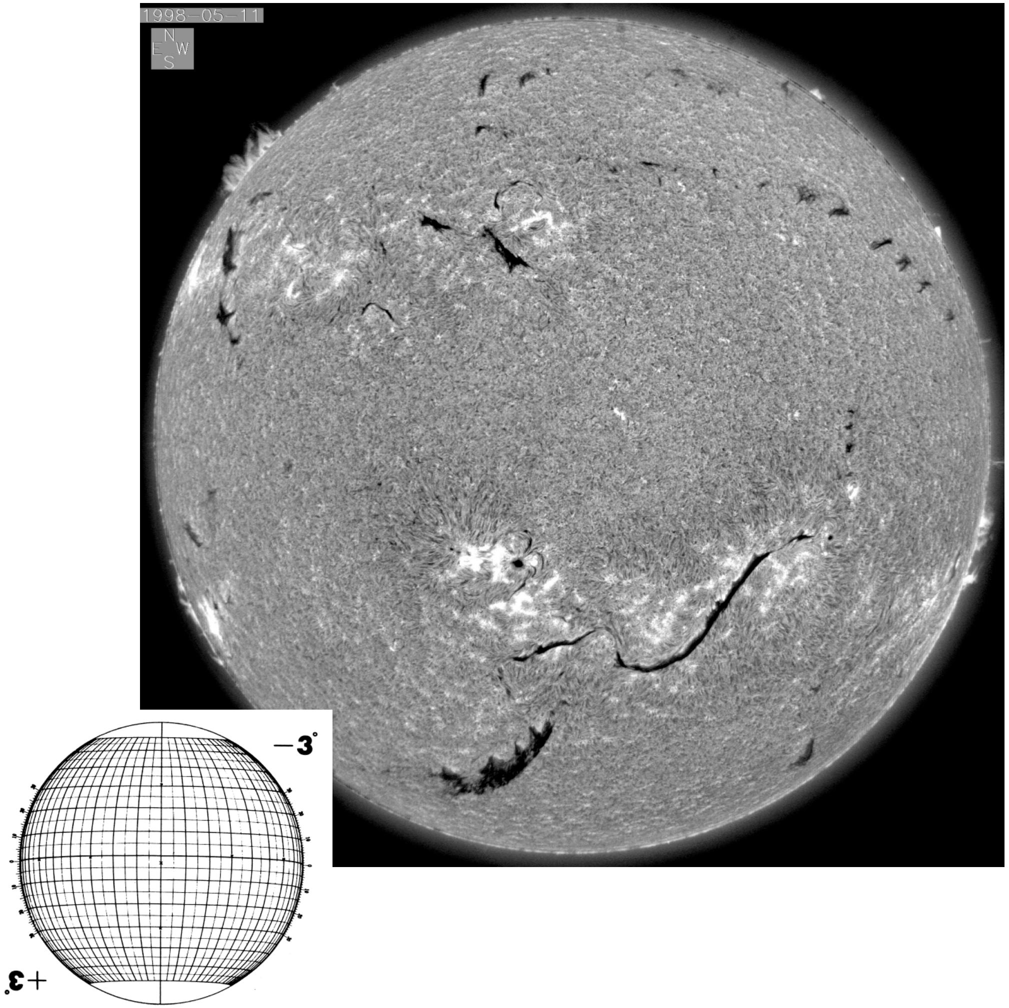

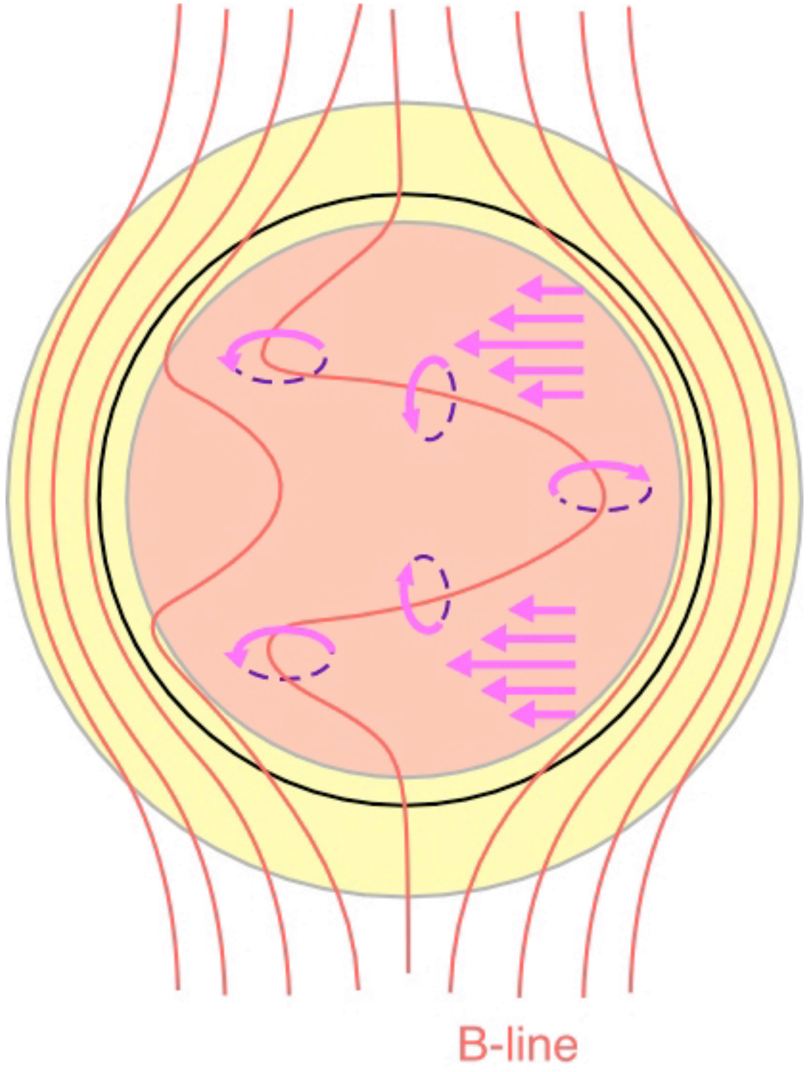

Zonal Flow in Rotational System --> Rossby wave

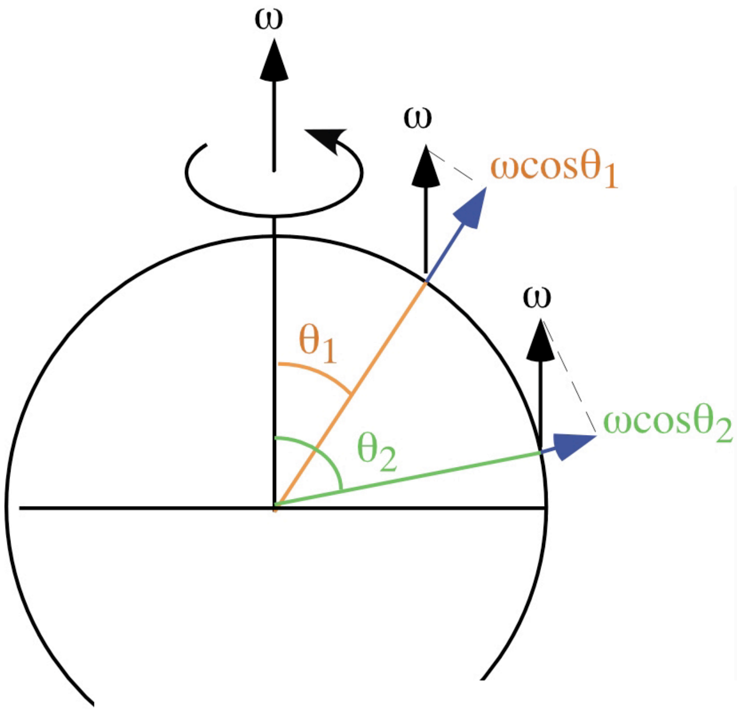

momentum equation

$$\rho\left(\frac{\partial \mathbf{V}}{\partial t}+\mathbf{V}\cdot\nabla\mathbf{V}\right)=-\nabla p-2\rho\boldsymbol{\omega}\times\mathbf{V}+\rho\mathbf{g}-\rho\boldsymbol{\omega}\times(\boldsymbol{\omega}\times\mathbf{r})+\mathbf{J}\times\mathbf{B}$$

or

$$\frac{\partial \mathbf{V}}{\partial t}=-\frac{\nabla p}{\rho}-\nabla\left(\frac{V^2}{2}\right)-[(2\boldsymbol{\omega}+\boldsymbol{\Omega})\times\mathbf{V}]+\mathbf{g}_e+\frac{\mathbf{J}\times\mathbf{B}}{\rho}$$

where

$$\boldsymbol{\Omega}=\nabla\times\mathbf{V},\quad \mathbf{g}_e=\mathbf{g}-\boldsymbol{\omega}\times(\boldsymbol{\omega}\times\mathbf{r})$$

Stable

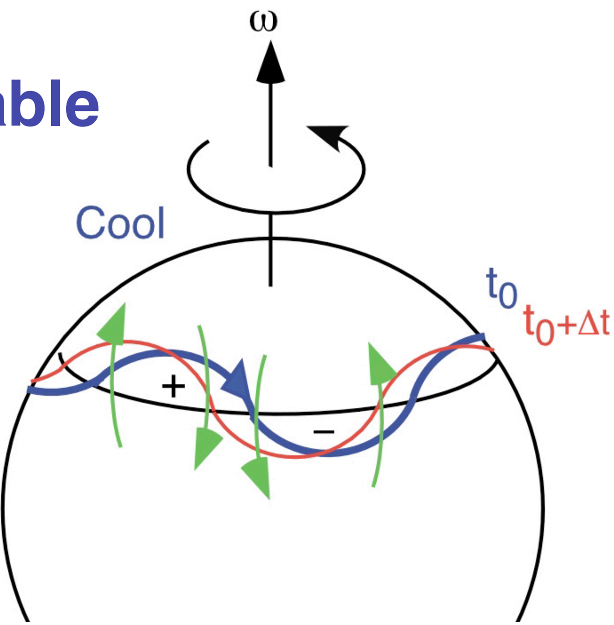

Unstable

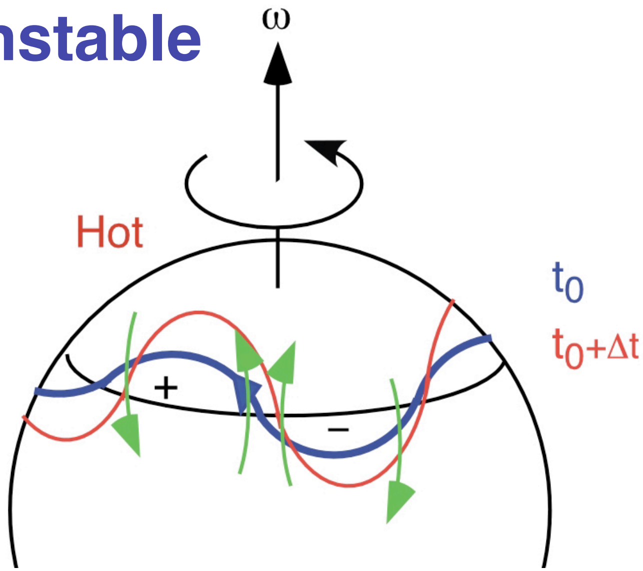

Laboratory simulation of general circulation (1)

Holton (1992): This is not a Rossby wave, because wis uniform in this case.

Fultz & Spence, 1967.

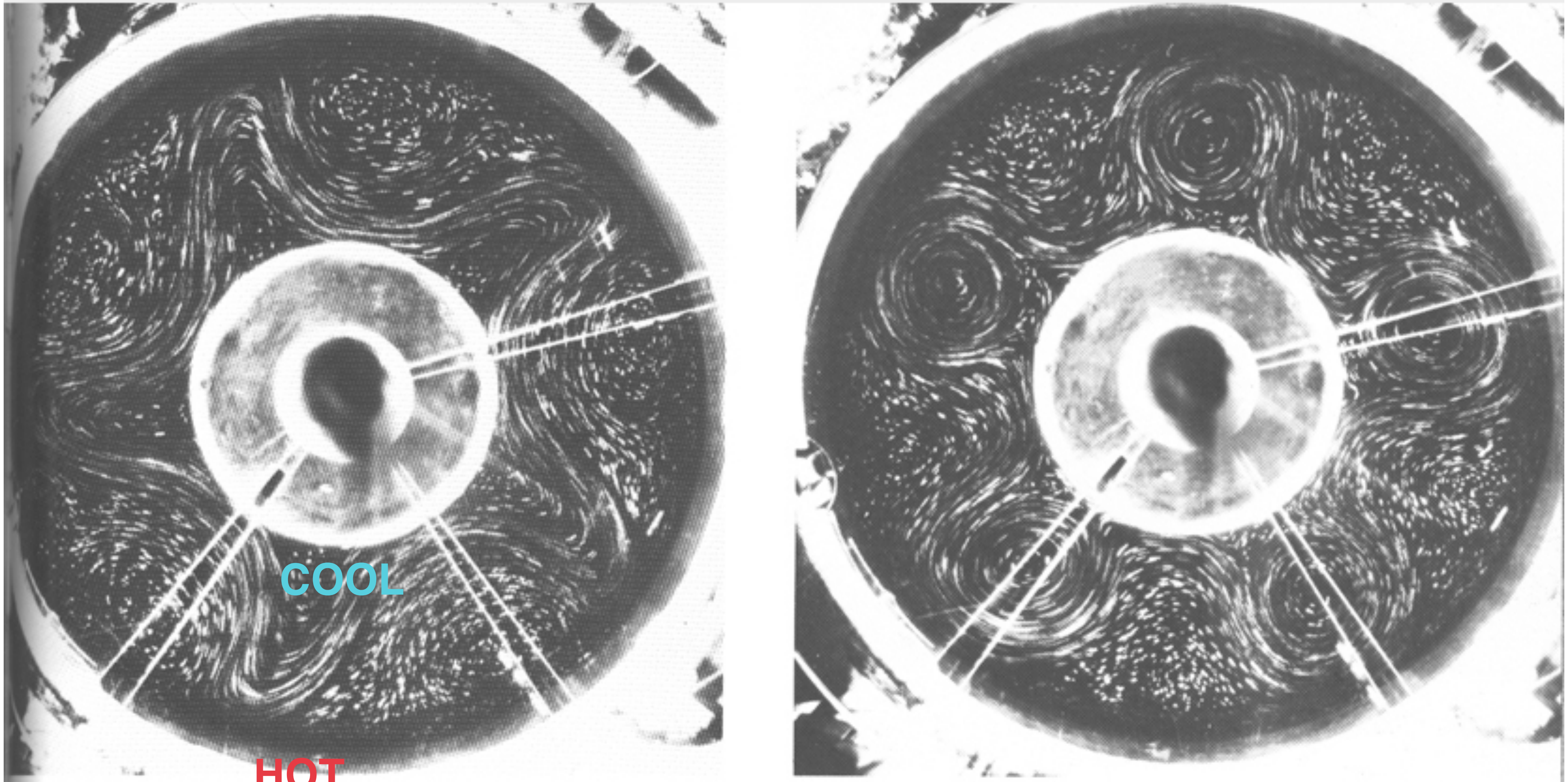

Heating: 80W at the rim and 15 W from a base ring.

Laboratory simulation of general circulation (2)

Holton (1992): This is not a Rossby wave, because wis uniform in this case.

Koschmieder, 1972.

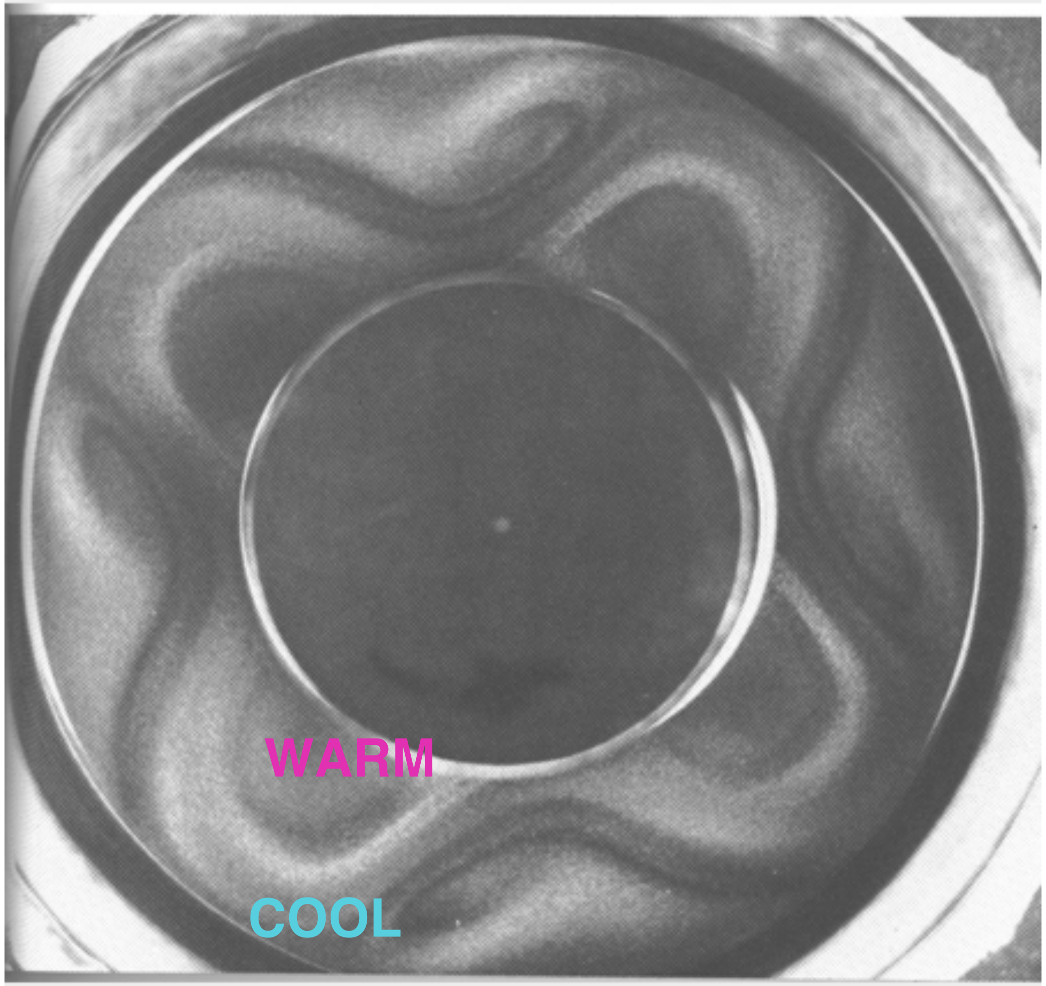

The core is 15 degrees warmer than the rim.

e.g., Solar convection zone

Formation of Rossby wave and Alfven waves in the coronal hole and boundary of coronal hole region

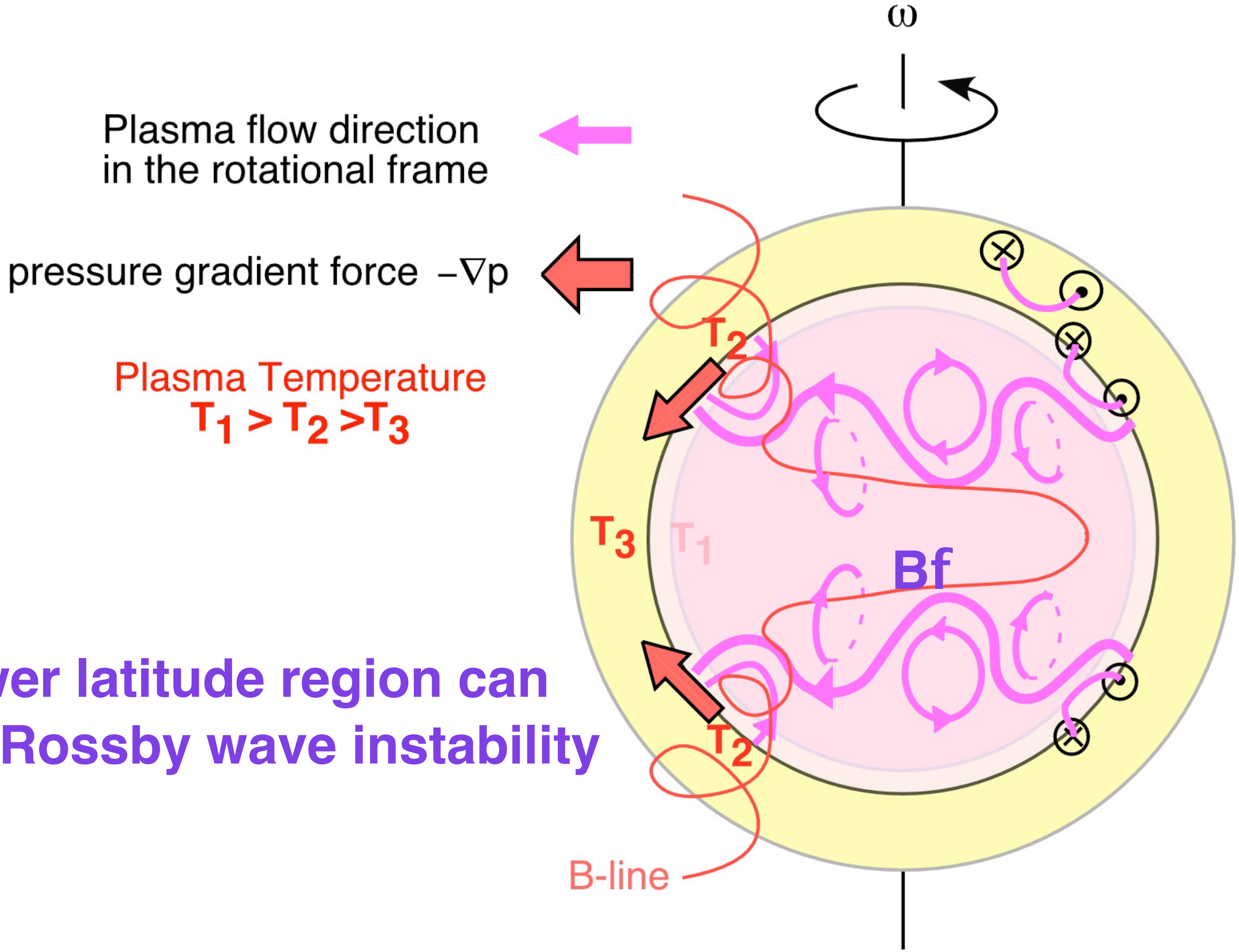

Bf in lower latitude region can stabilize Rossby wave instability

Rossby wave: Hα observation of solar filaments (02/22/1998)

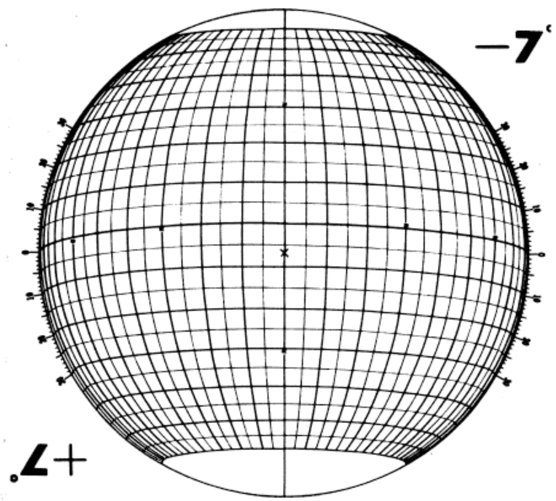

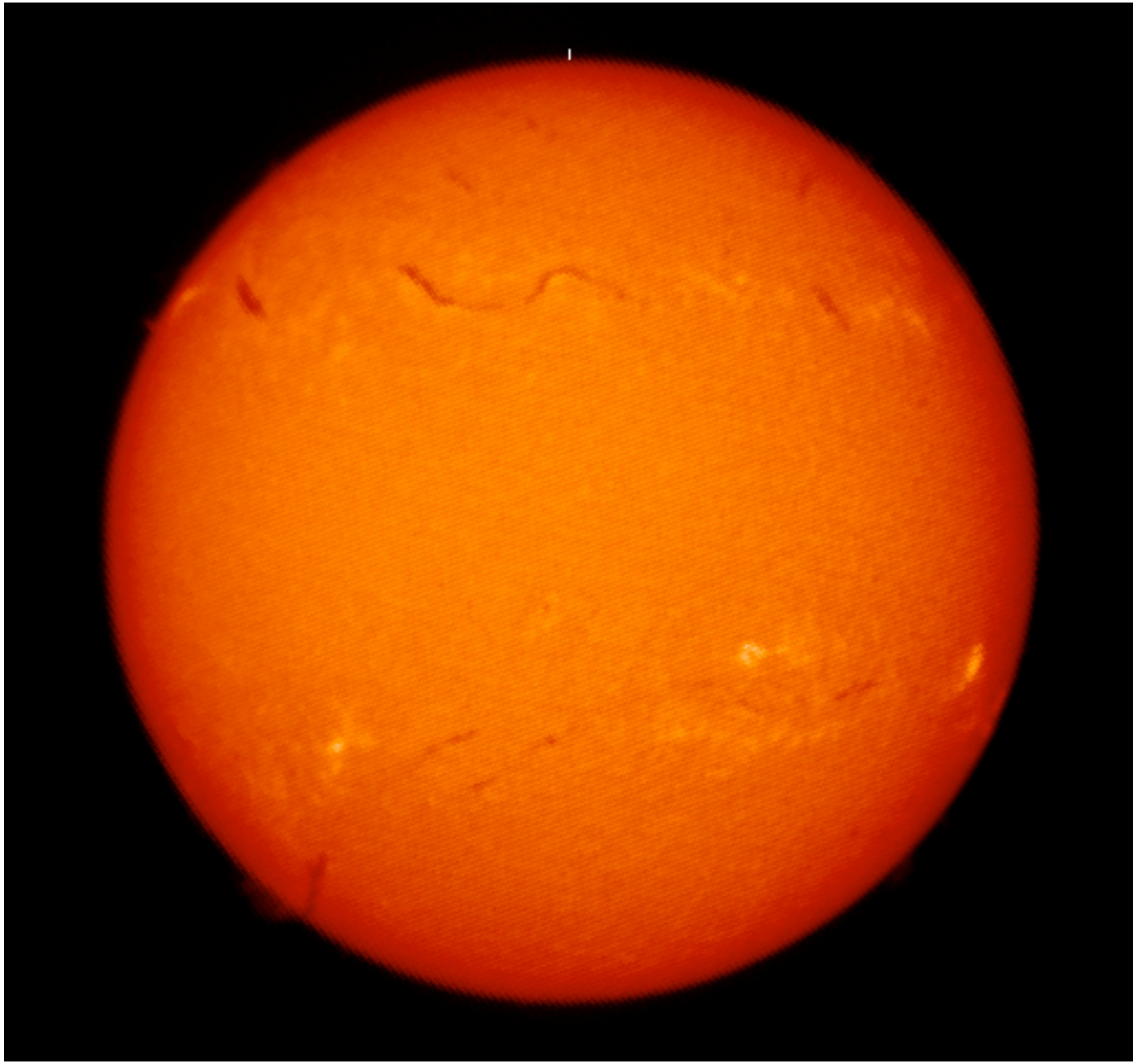

Rossby wave: MDI observation of solar magnetic field (02/22/1998)

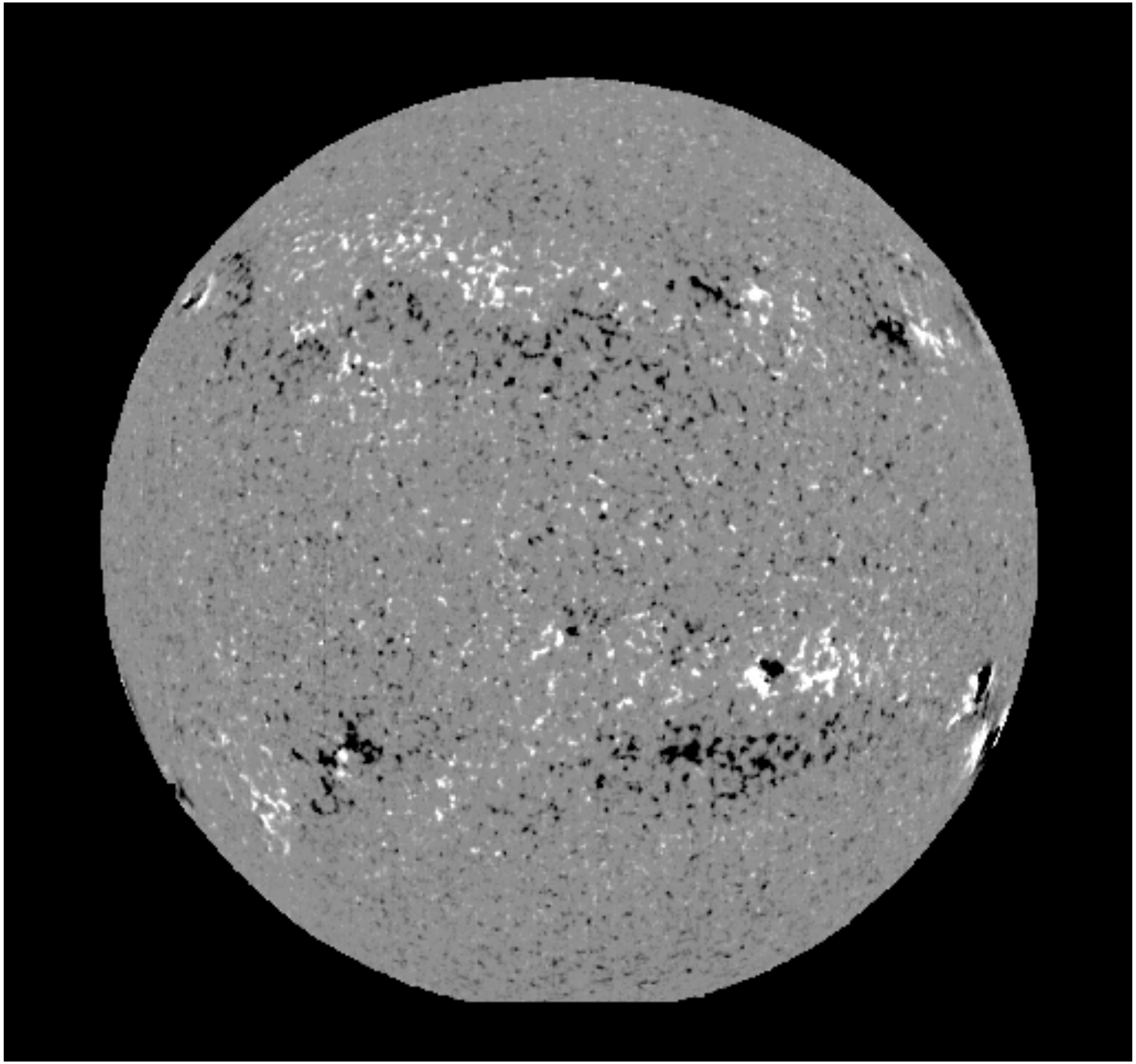

Rossby wave:
Yohkoh SXT observation
07/05/1998

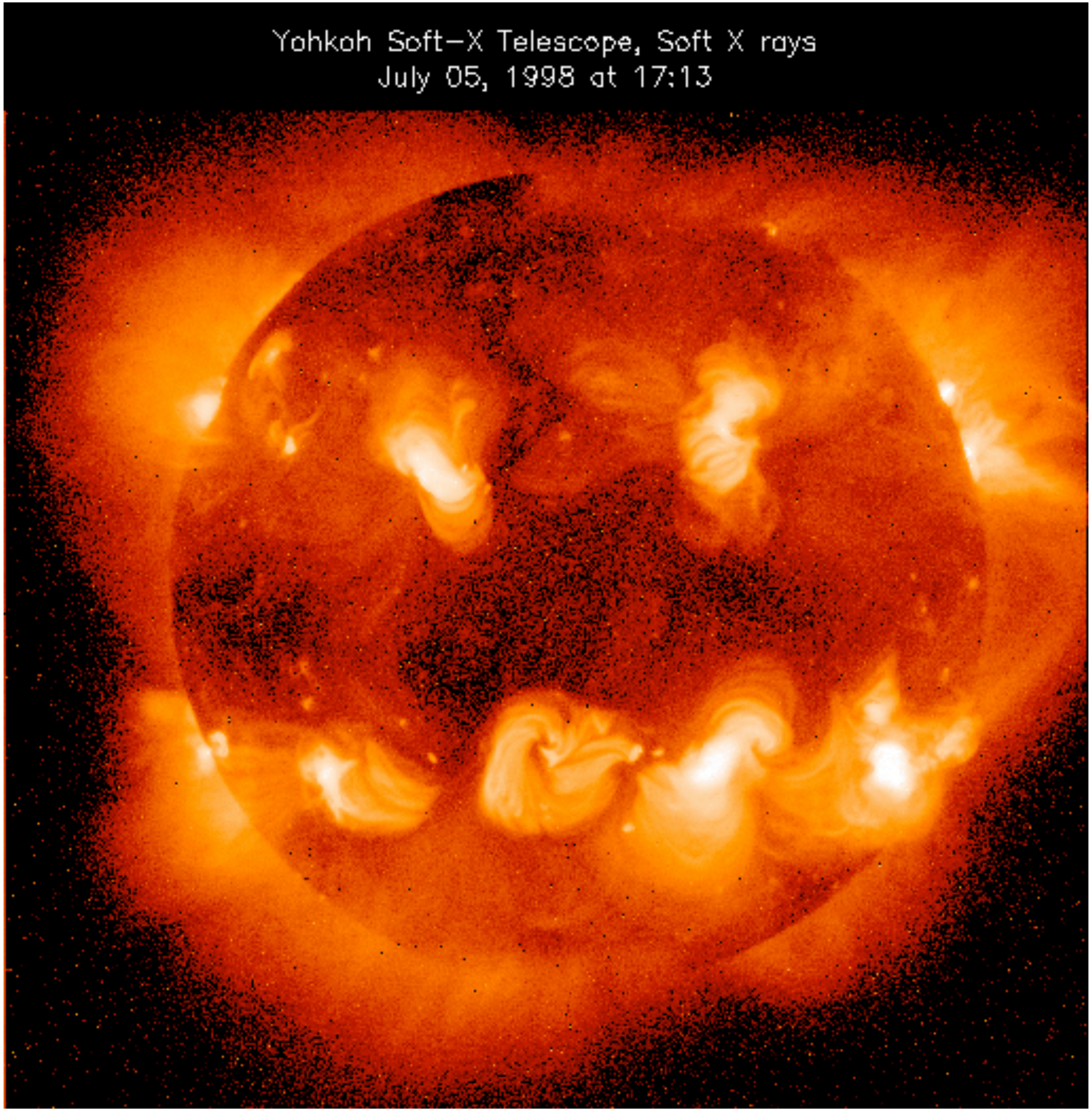

Nonlinear Evolution of Rossby Wave Lead to Formation of Elephant-trunk Coronal Hole

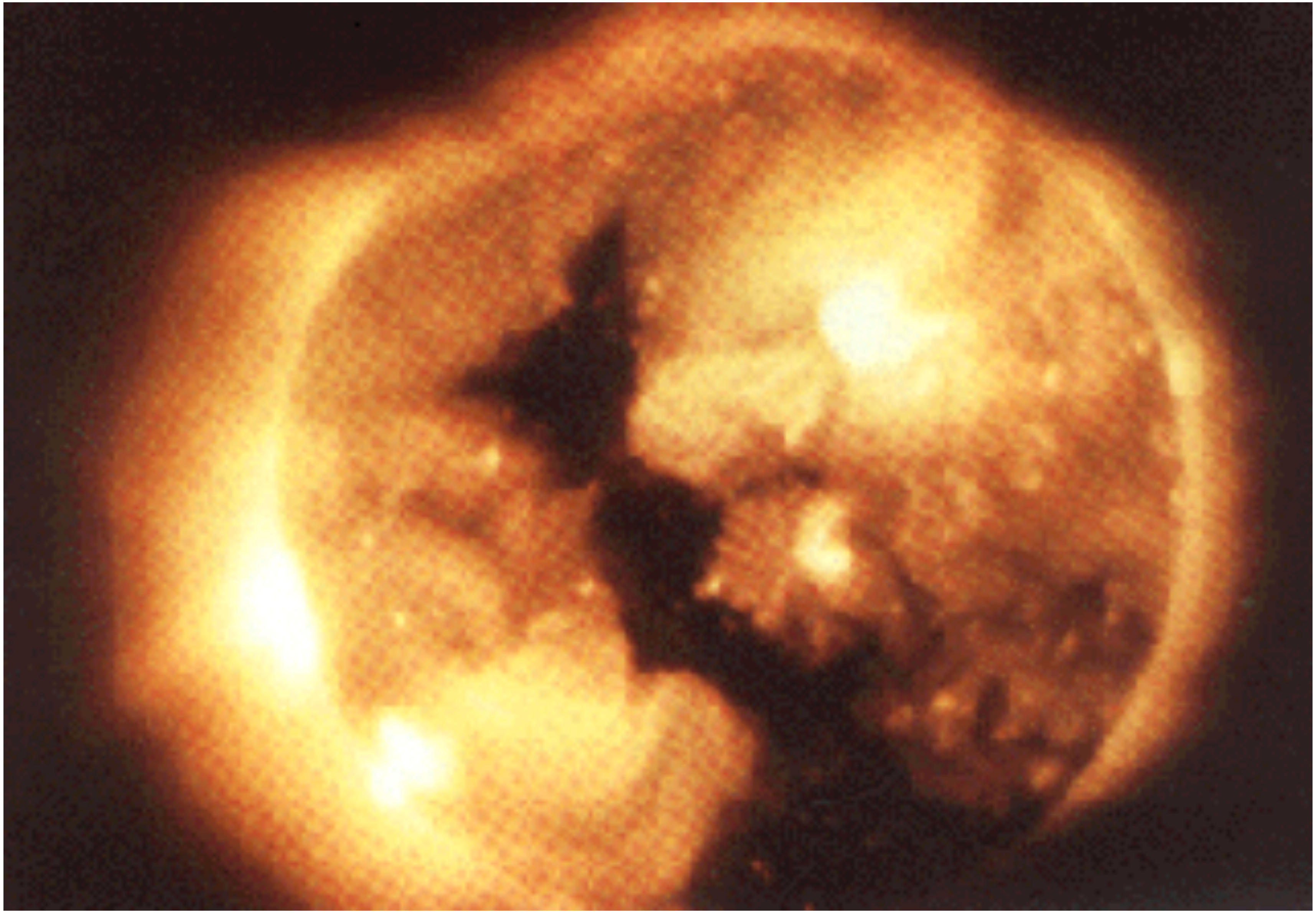

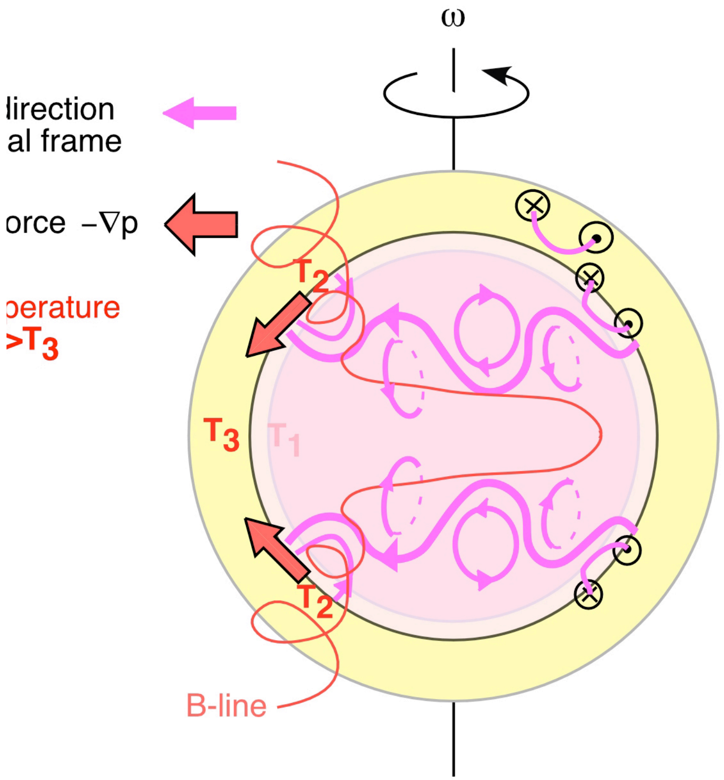

Generation of large amplitude, nearly circularly polarized Alfven waves in the coronal hole region

MDI Observation of Solar Differential Rotation
Red: faster, Blue: slower

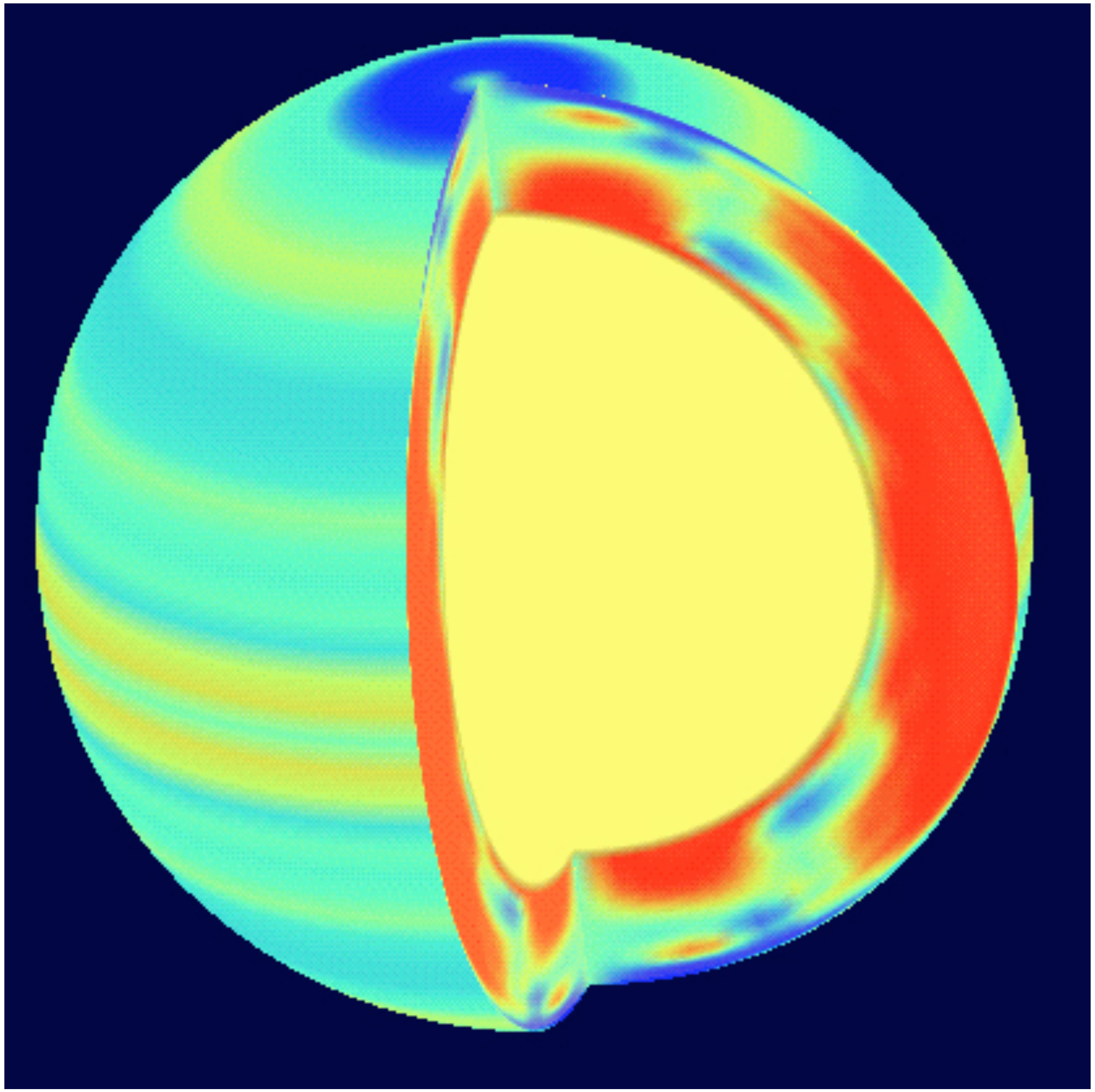

Ulysses observation of solar wind speed(1991-1998)

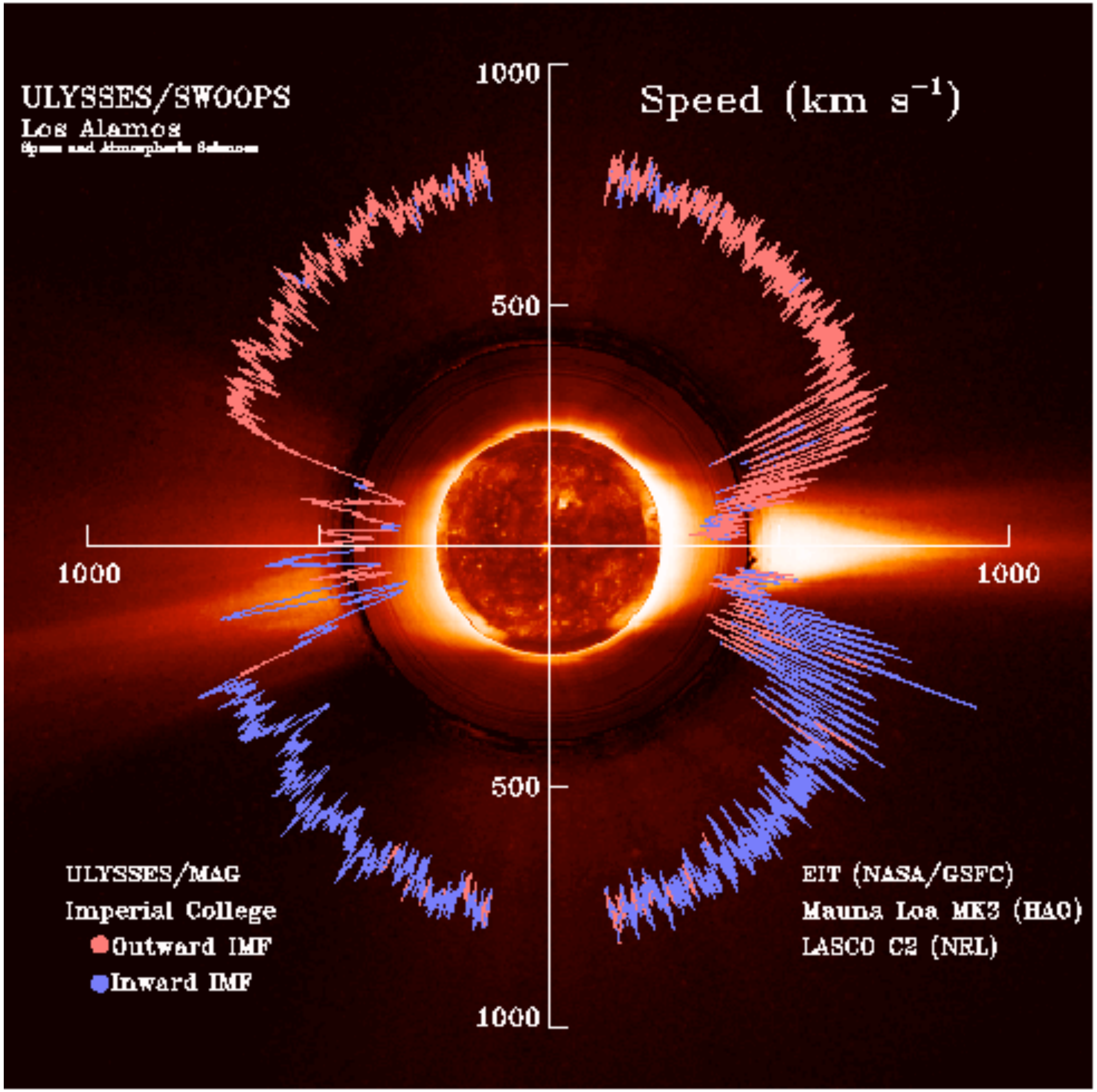

It is believed that …
observed large-amplitude Alfven waves are responsible for solar wind acceleration in the polar coronal hole

Q: What is the energy source of these large-amplitude Alfven waves?

A: Rossby wave!

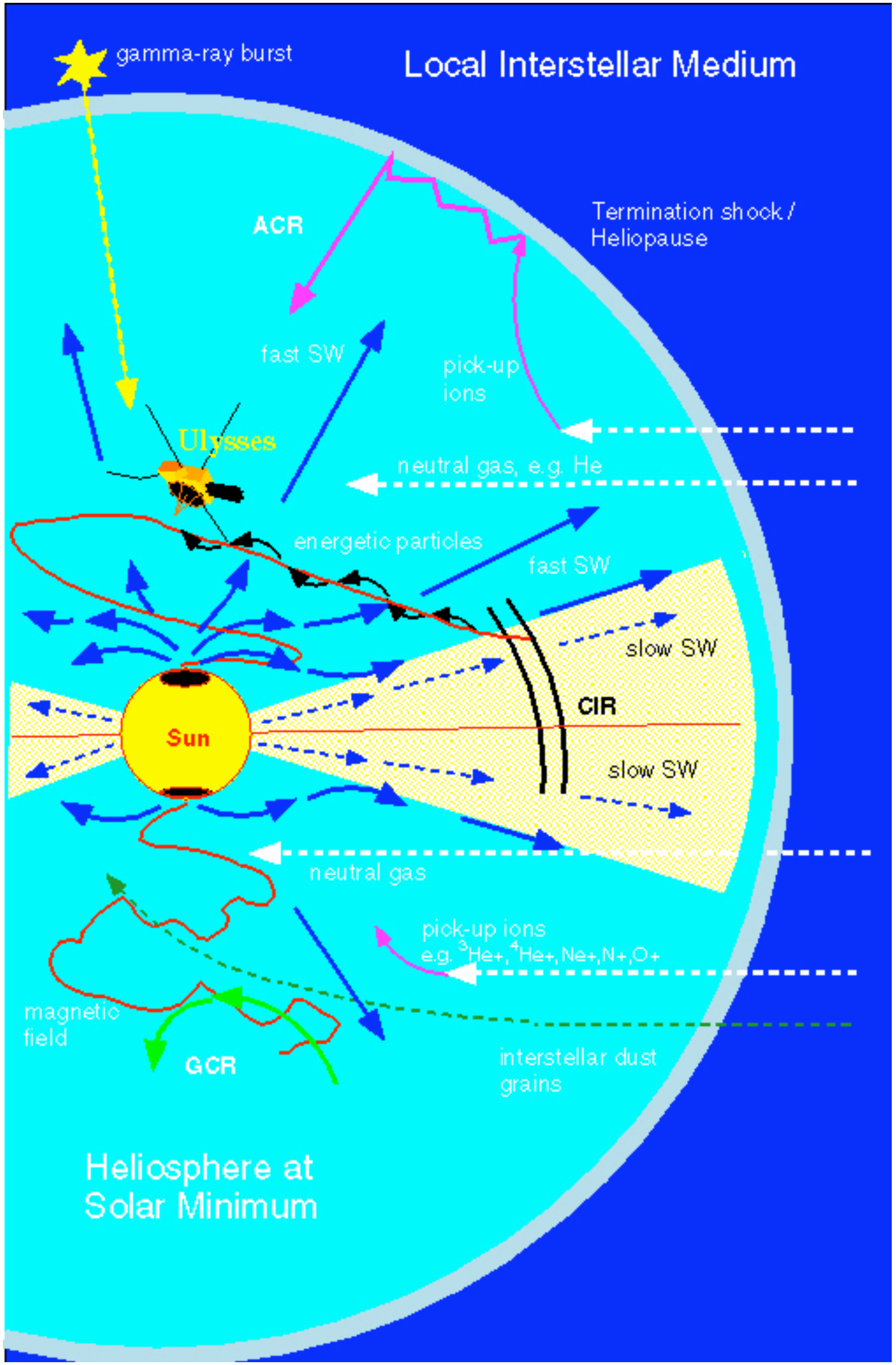

Rossby wave on the Sun can result in plane polarized Alfven wave in the solar wind

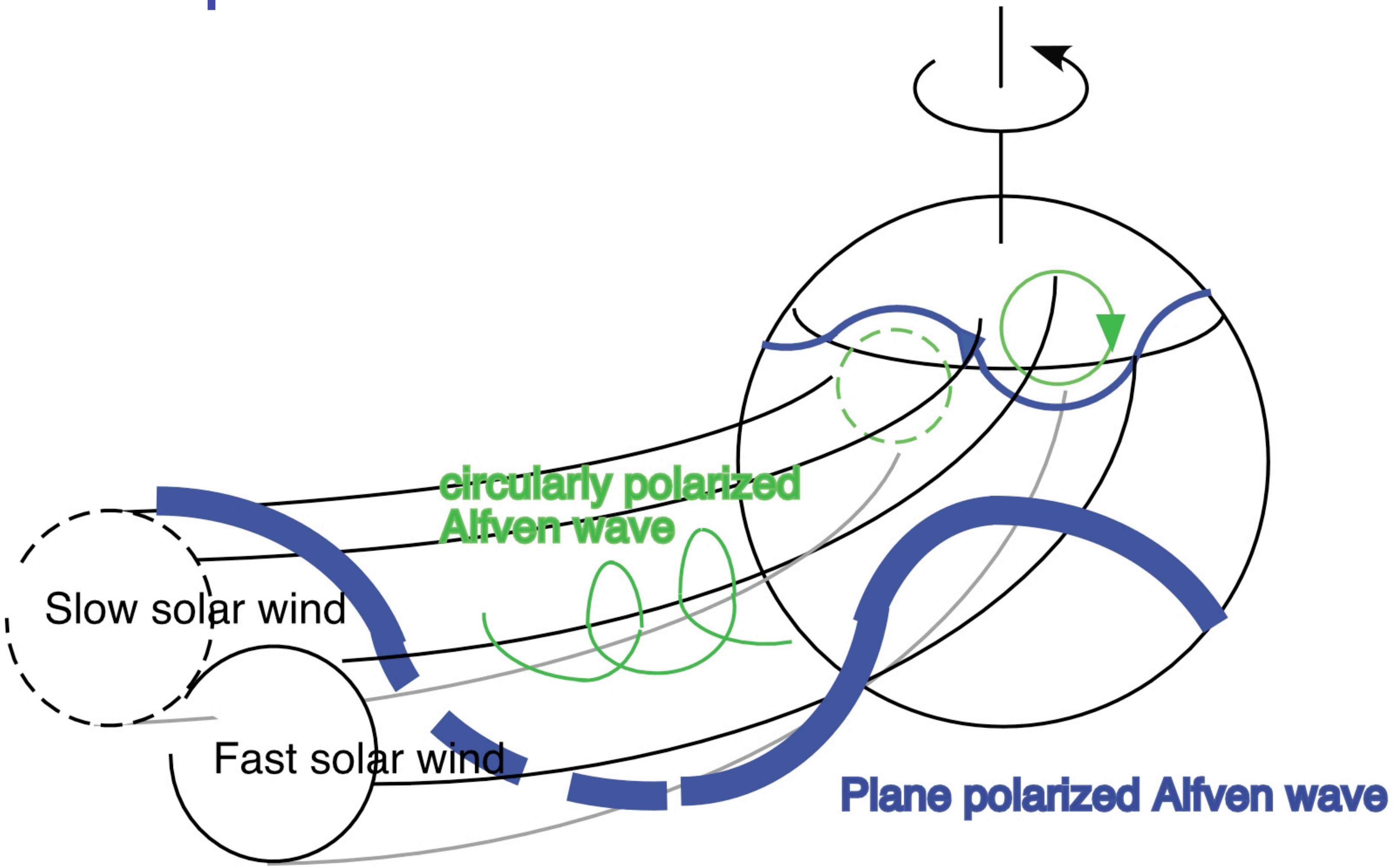

Theoretical Solutions of Steady State Nonlinear Alfven Waves and Rotational Structure in Ion-Electron Two-Fluid Plasma

(Lyu and Kan, 1989)
(Lyu, 1991)

Observation of Plane Polarized Alfven Waves in the Solar Wind
--- Evidence of Rossby wave on the Sun

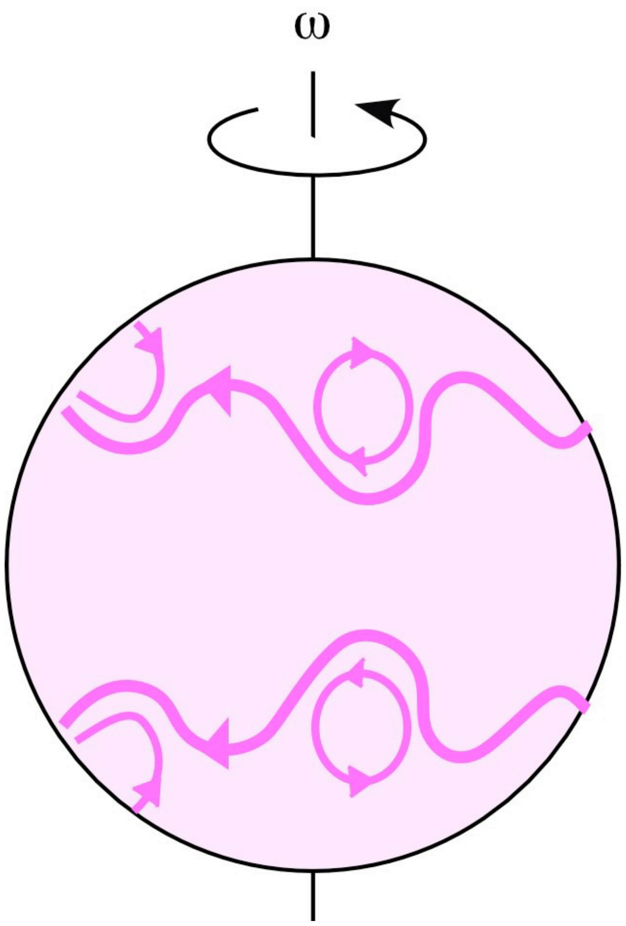

Magnetic hodograms of Alfven waves and rotational discontinuities (RDs)

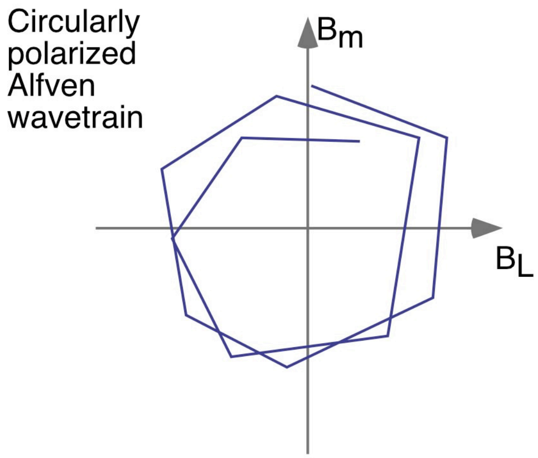

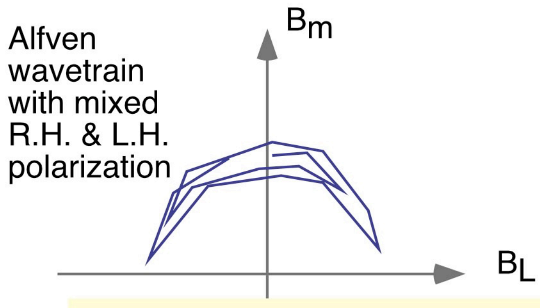

Planar polarized Alfven waves (i.e., waves with mixed polarization) have been observed by Pioneer 10 and Pioneer 11 at 5 AU and 2.5 AU, respectively.
(Mavromichalaki et al., 1988)

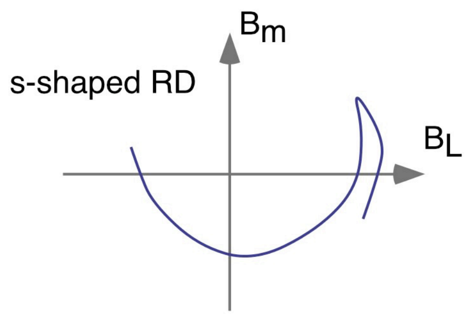

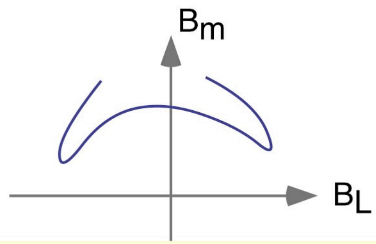

double-hooked RD
(e.g., Neugebauer and Buti, 1990)

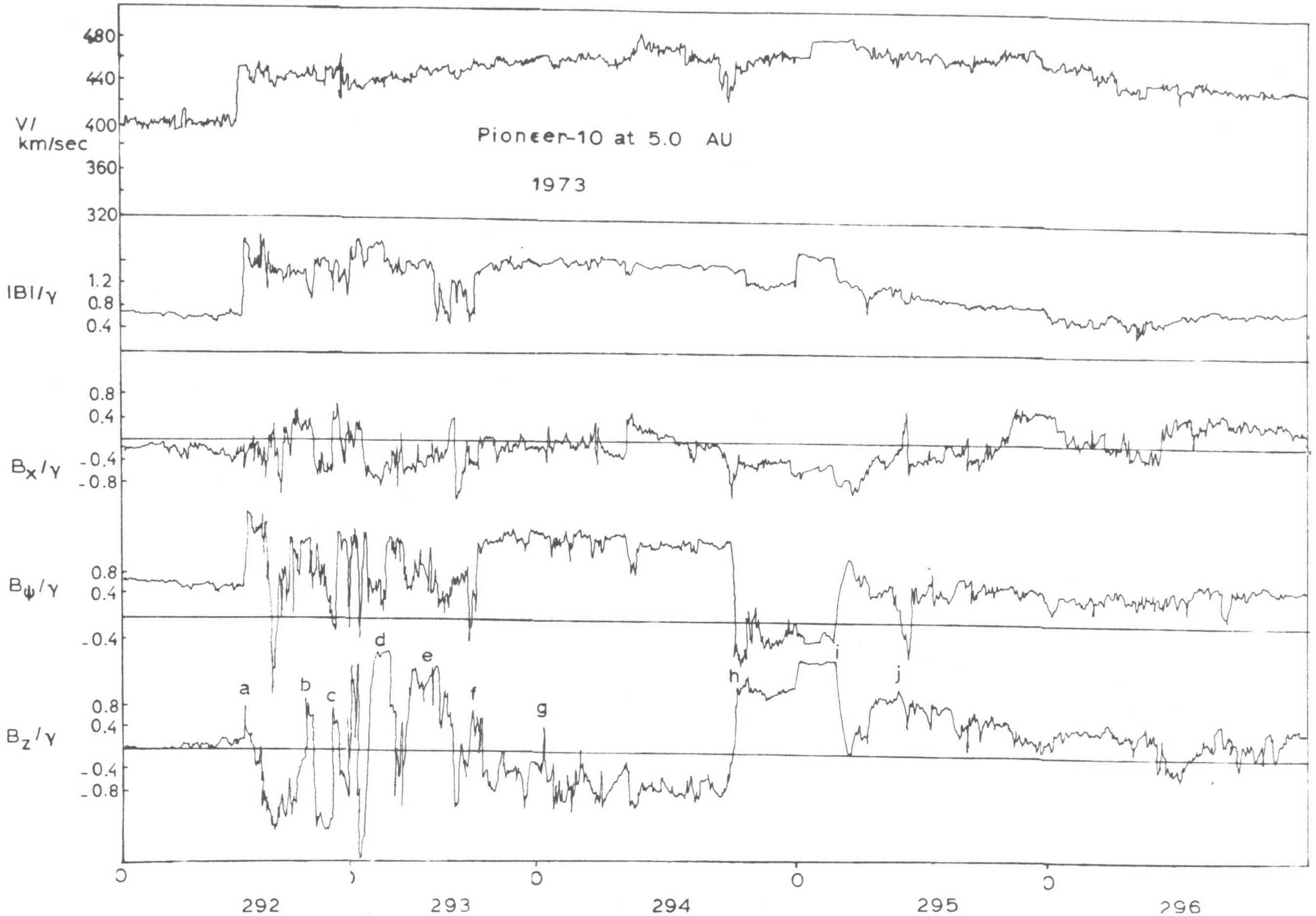
V/
km/sec
480
440
400
360
320
Pioneer-10 at 5.0 AU
1973
IBI/γ
1.2
0.8
0.4
0.8
0.4
$B_x/γ$
-0.4
-0.8
$B_ψ/γ$
0.8
0.4
-0.4
a
b
c
d
e
f
g
h
i
j
$B_z/γ$
0.8
0.4
-0.4
-0.8
292
293
294
295
296

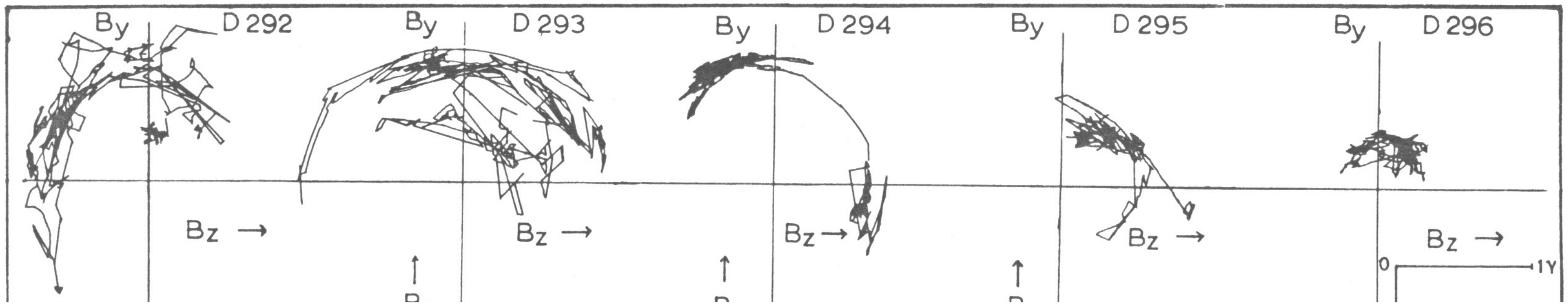
By
D 292
By
D 293
By
D 294
By
D 295
By
D 296
Bz →
Bz →
Bz →
Bz →
Bz →
0
1γ

RELATIVELY STABLE, LARGE-AMPLITUDE WAVES SEEN AT 2.5 AND 5.0 AU

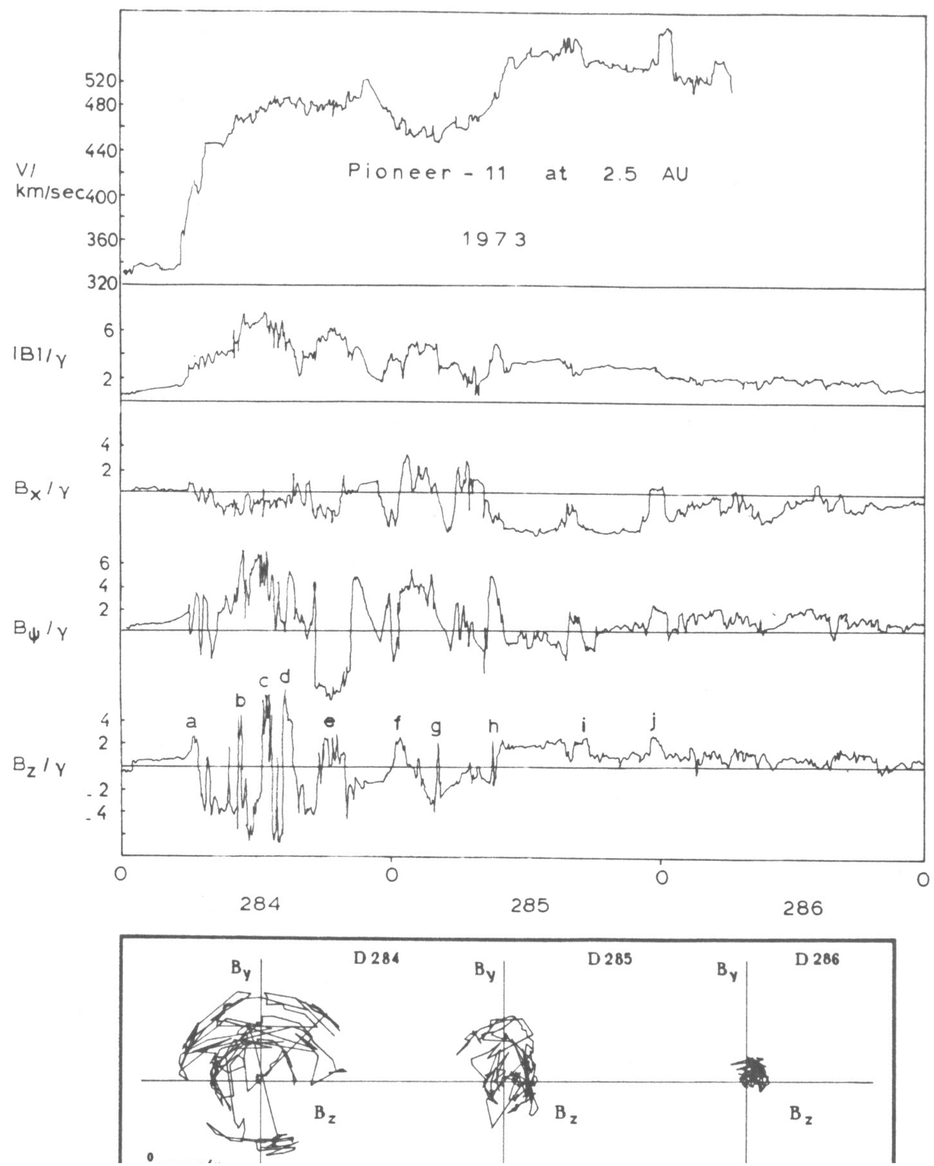

Mavromichalaki et al., 1988

Conclusion

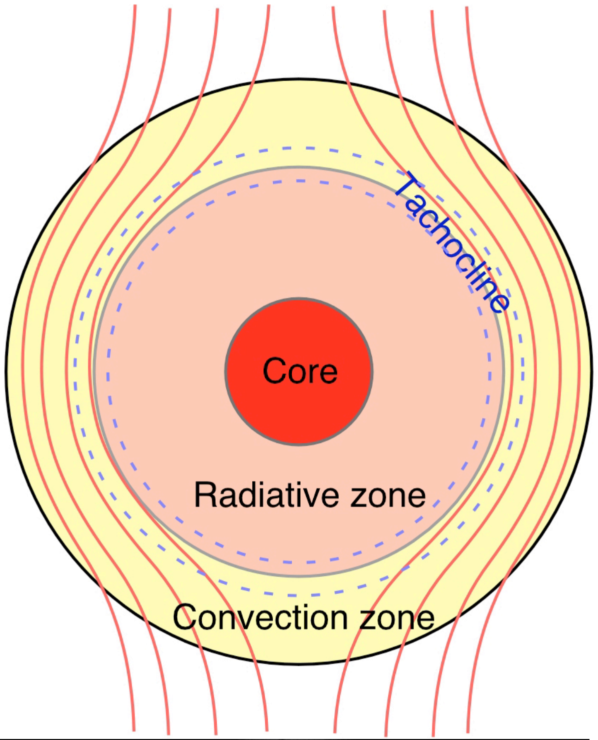

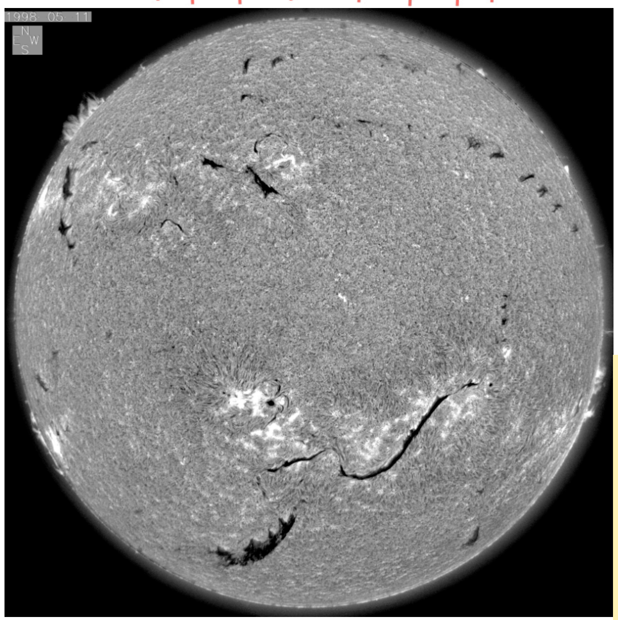

BBO Hα observation 05/11/1998

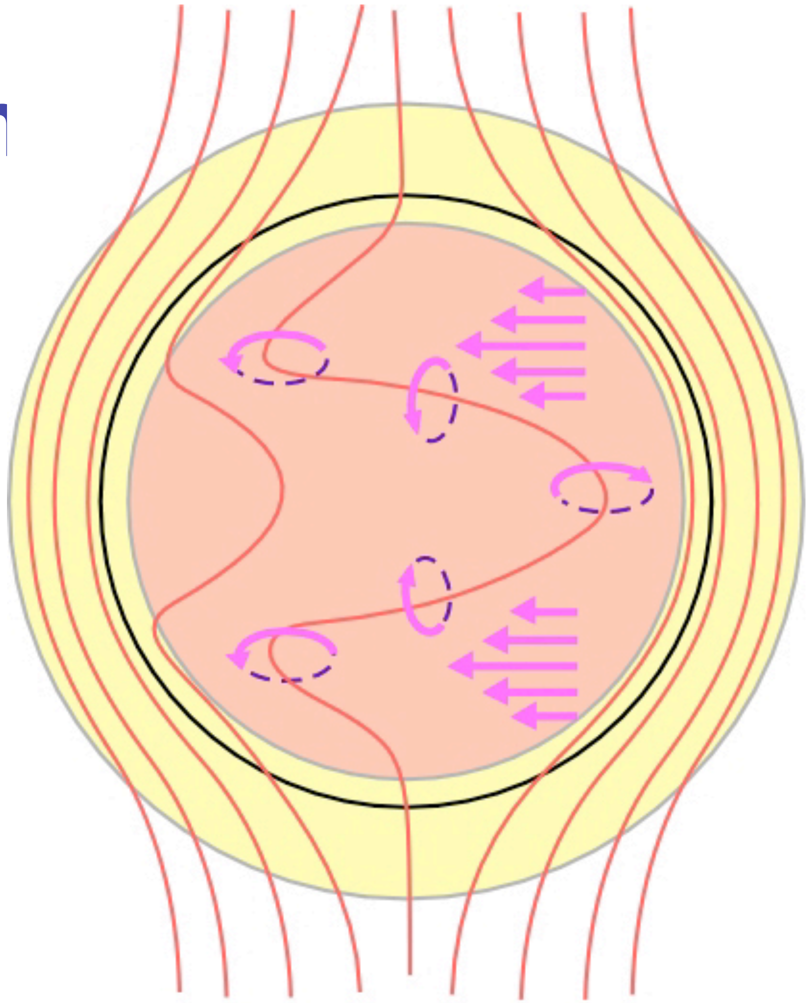

Our Model:

Plasma in solar convection zone has

Higher Temperature in the Polar Region

Easterly Wind ==> Differential Rotation

Discussion:

Cause of Maunder Minimum and variations in solar activities:

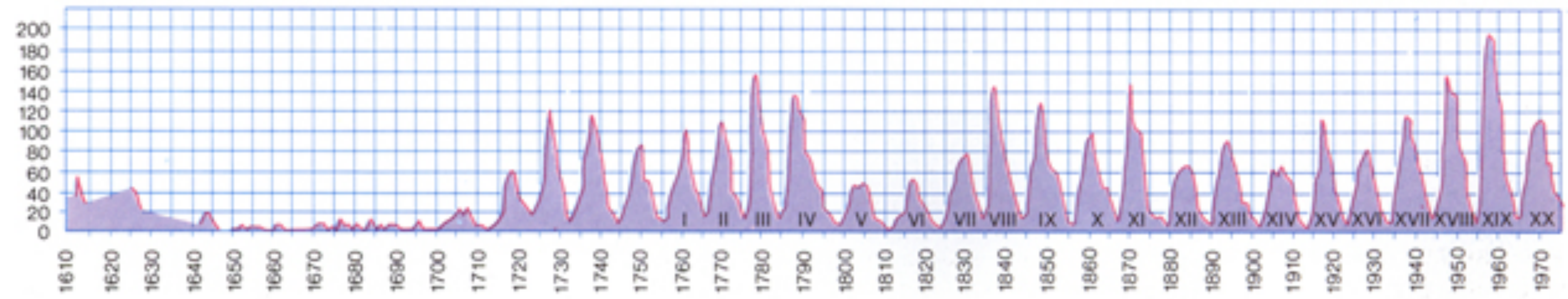

Gravitational disturbances and/or tidal effects

>> reduce density gradient (in the tachocline region)
>> reduce diamagnetic current
>> reduce temperature gradient
>> reduce differential rotation
>> reduce solar activities
>> reduce sunspots number

Observations: (~ 90 years Gleissberg cycle) (tidal effect)

Sunspots number decreases with increasing solar diameter.

(Jupiter:11.86 yr.) (Saturn: 29.5 yr.) (Uranus: 84 yr.)

Part 2

Observation of Solar Surface Differential Rotation

TON data analysis

H. S. Yu, L. H. Lyu, D. Y. Chou

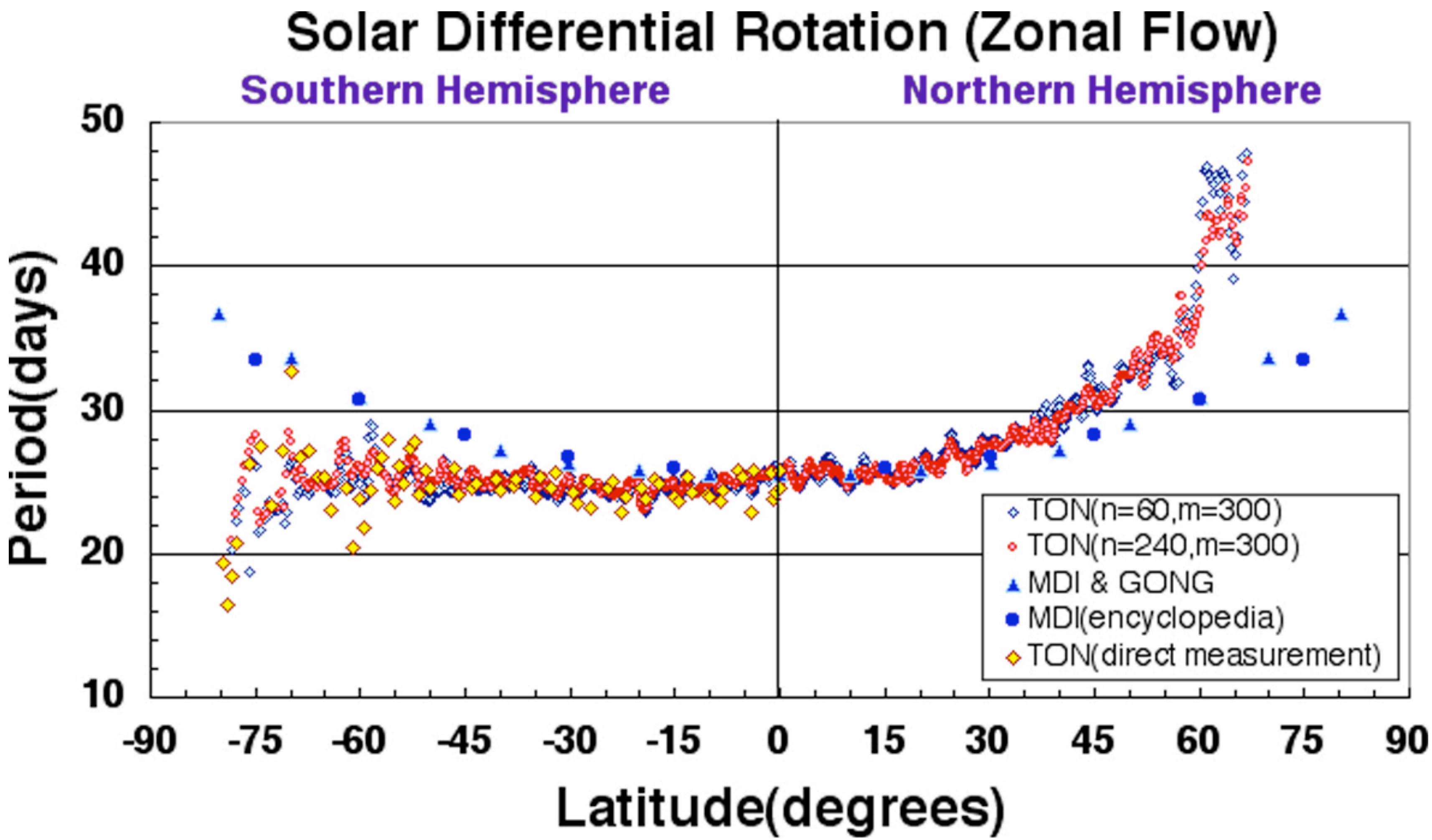

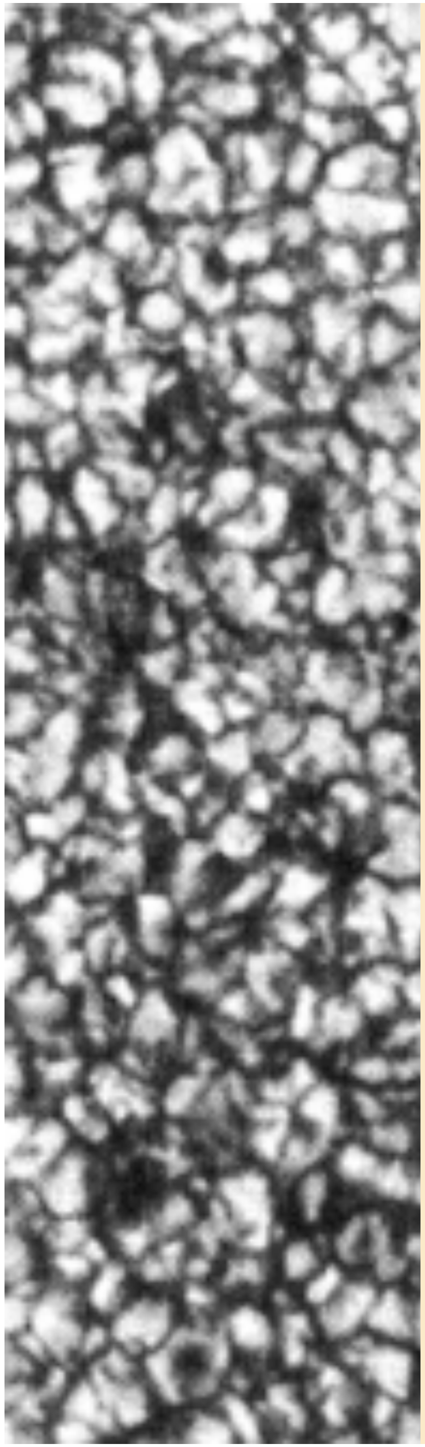

TON one-minute snapshot image (Granulations dominate)

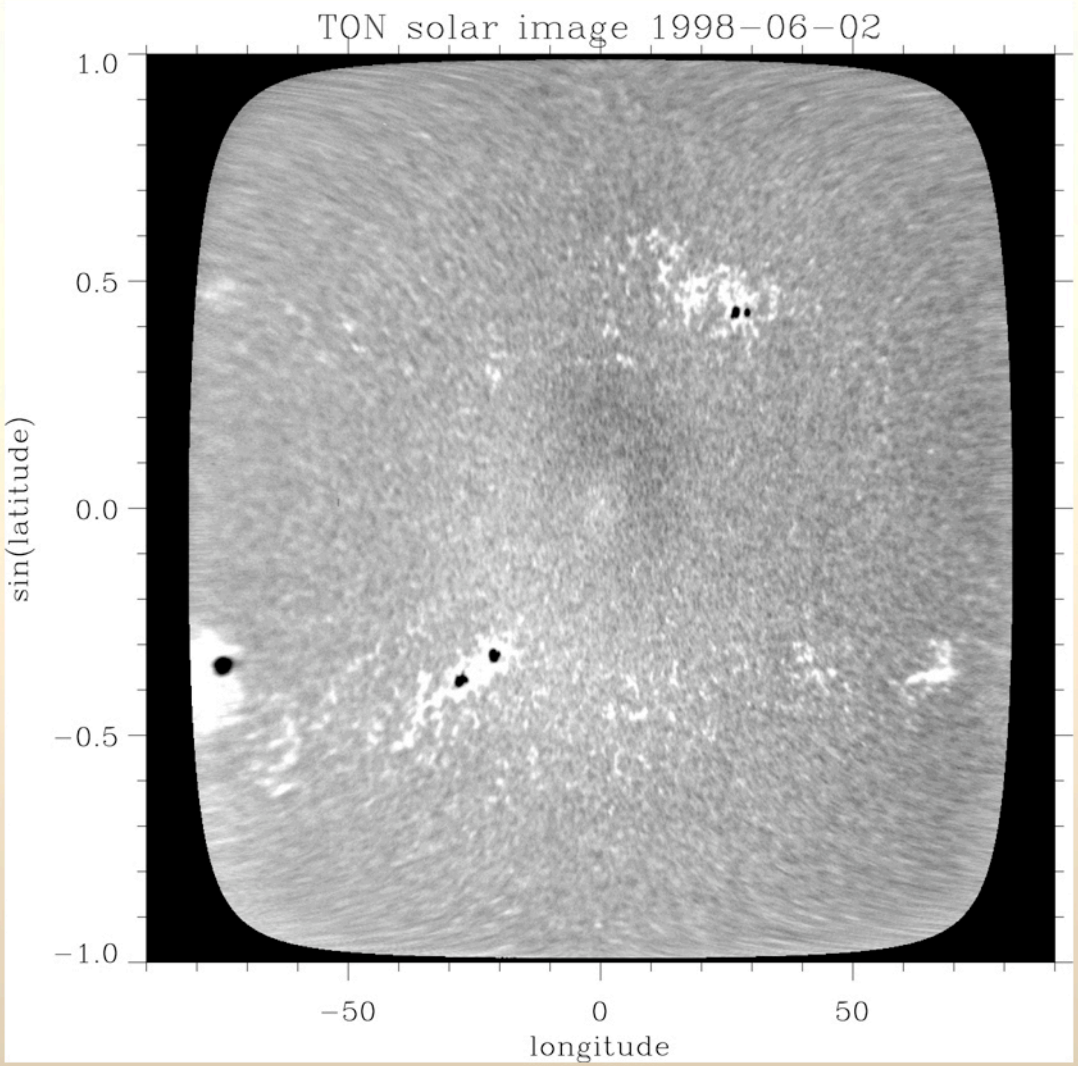

Time integrated (>500min) image (Supergranulations dominate)

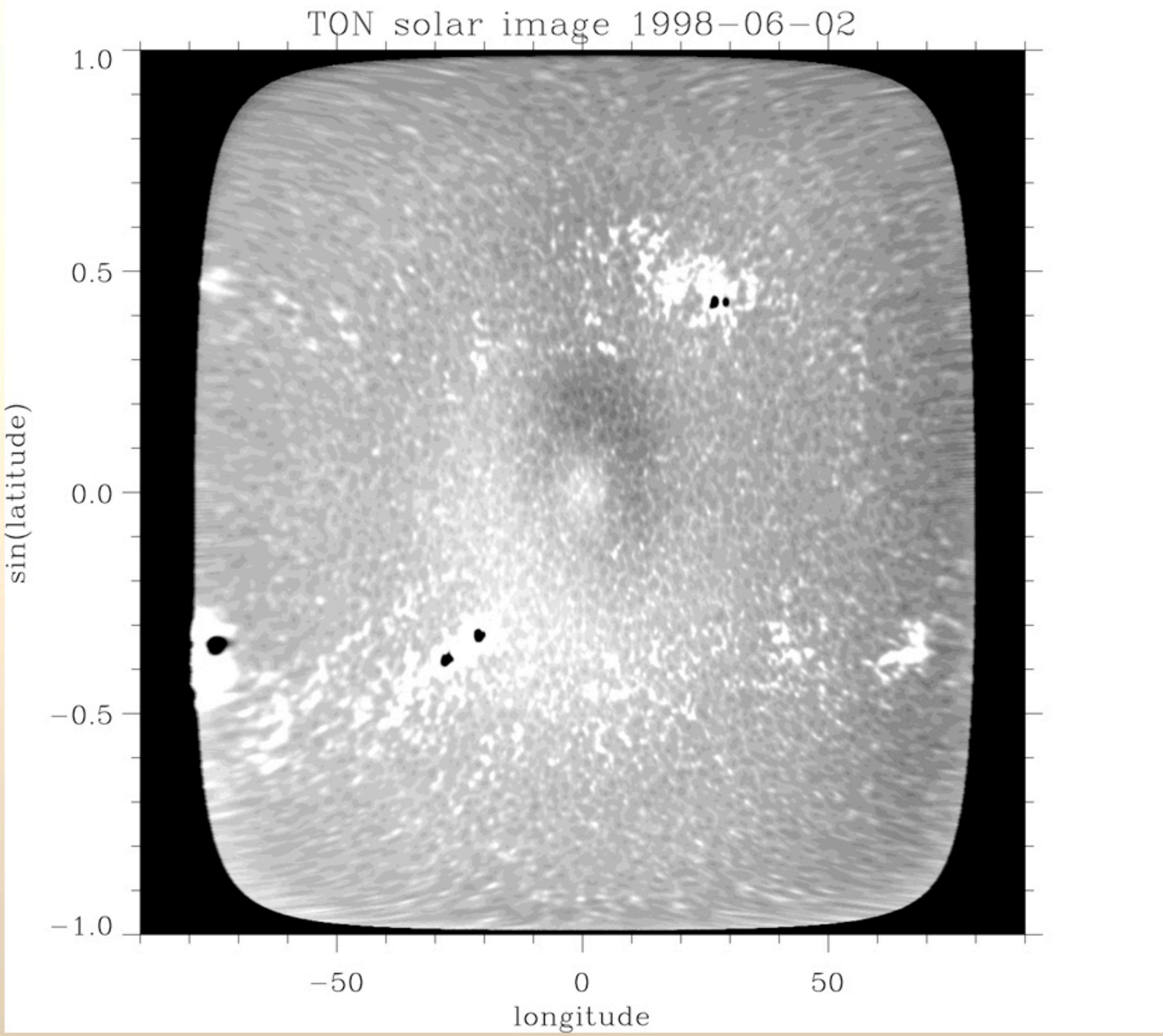

Direct measurement

at latitude=27°S

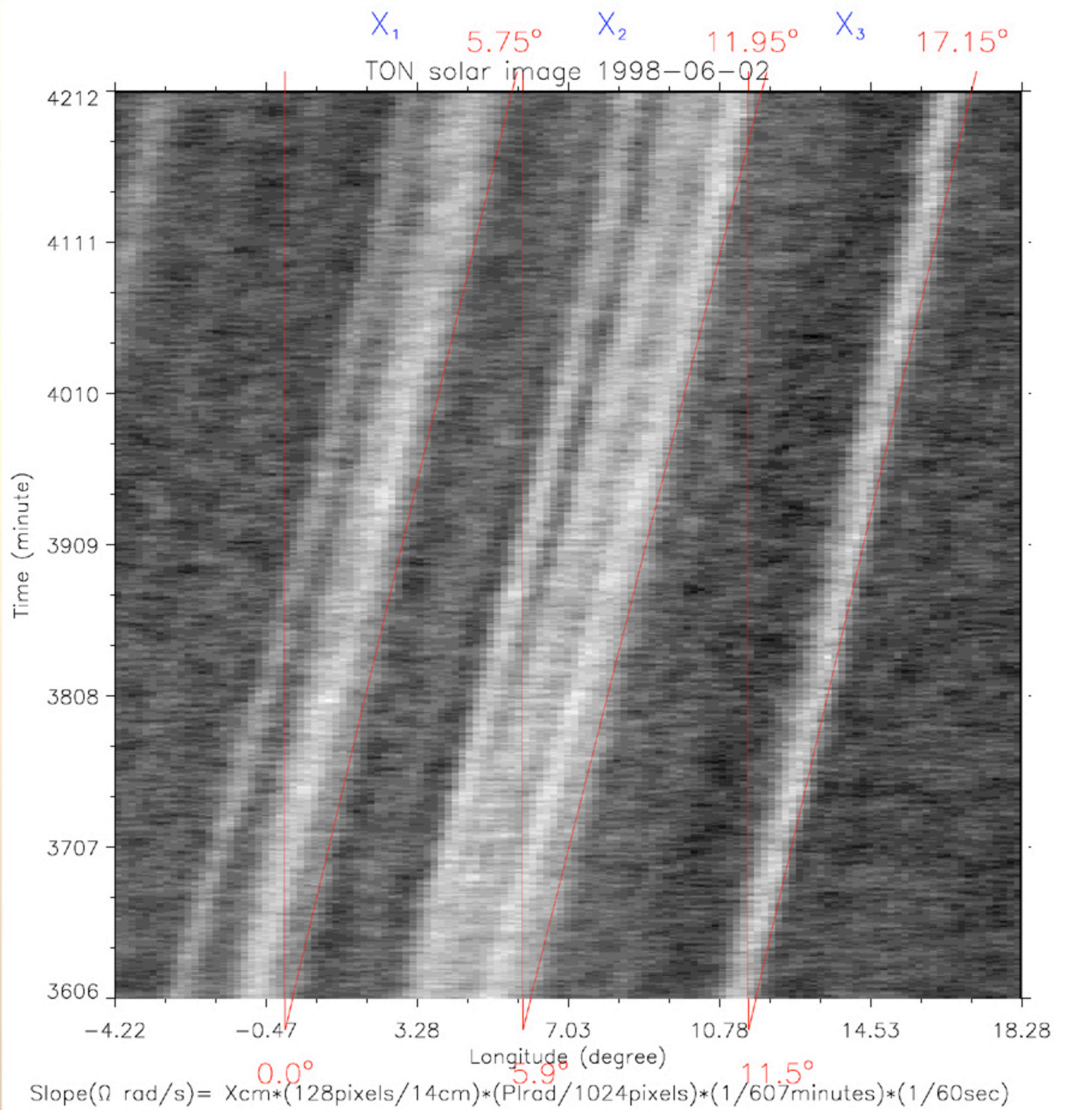

Correlation analysis

Let Fourier transform of function $h(x)$ to be $h(k) = \mathscr{F}[h(x)]$, where $h(x) \in R$ and $h(k) \in C$. It can be shown that if $h(x) = \int f(x')g(x-x')dx'$ then $h(k) = f(k) * g(k)$.
Likewise, if $h(x) = \int f(x')g(x'+x)dx'$ then

$$h^c(k) = f(k) * g^c(k) \qquad (1)$$

where $h^c(k)$ is the complex conjugate of $h(k)$.

To reduce numerical error, in our correlation analysis, data of given latitude and time at different longitude are shift and normalized based on their mean and standard deviation, respectively. Autocorrelation function $h(x)$ of given latitude can be obtained from $h^c(k)$, which can be obtained from Eq. (1).

We normalized correlation function $h(x)$ at different latitude by the maximum value $h(x)$ at the given latitude. We can then plot an image of the normalized $h(x)$ at different latitude. The peak distribution of $h(x)$ can be seen from the follow four panels.

h(x) before normalization

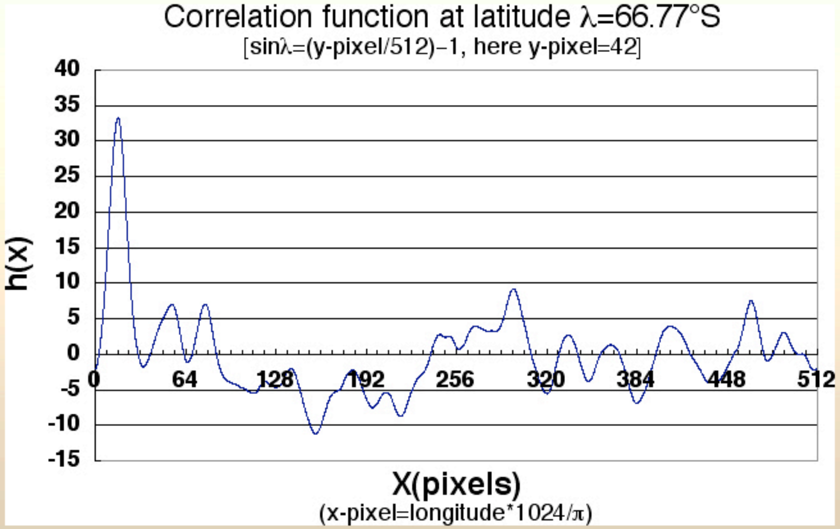

Normalized h(x)

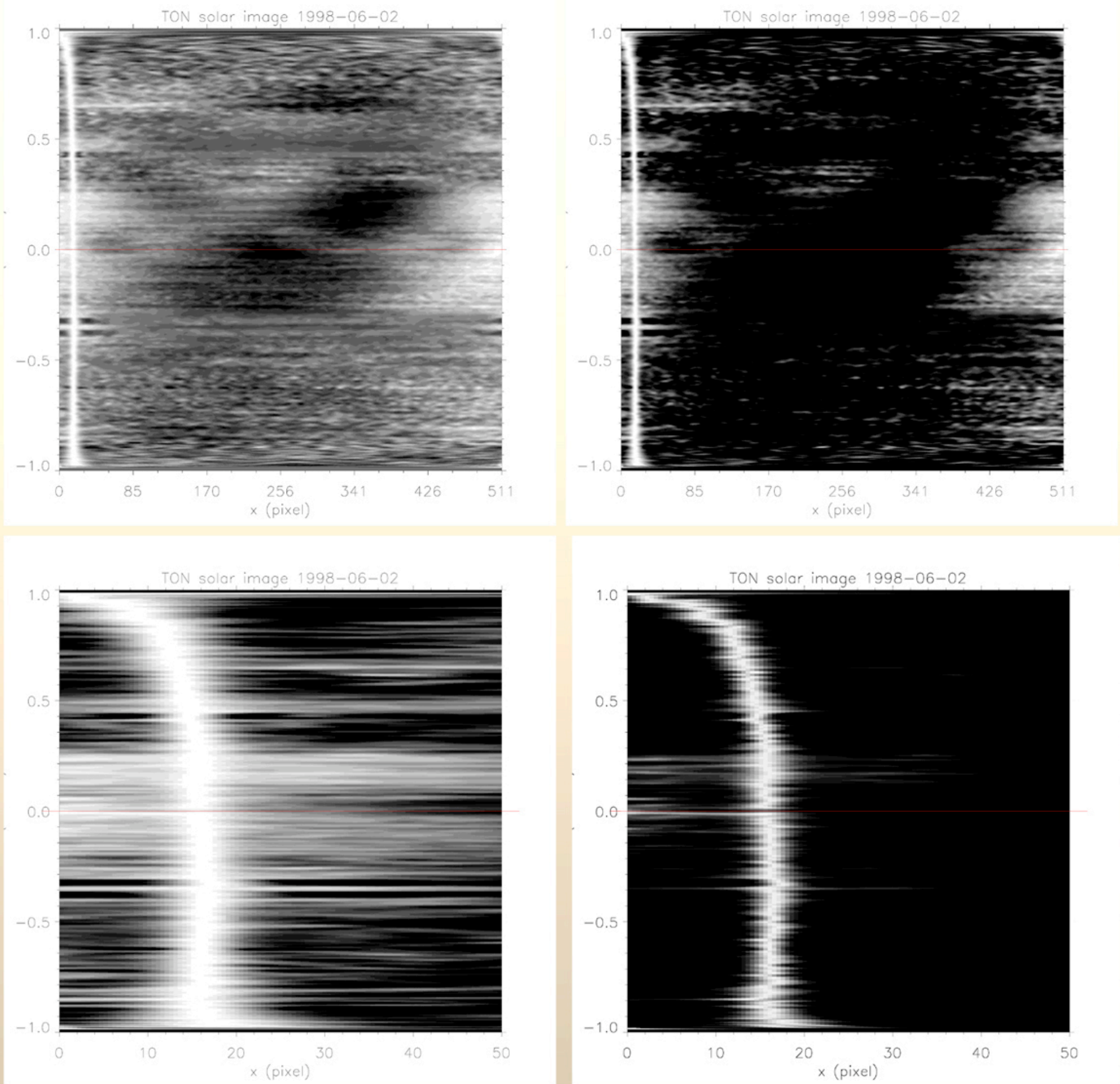

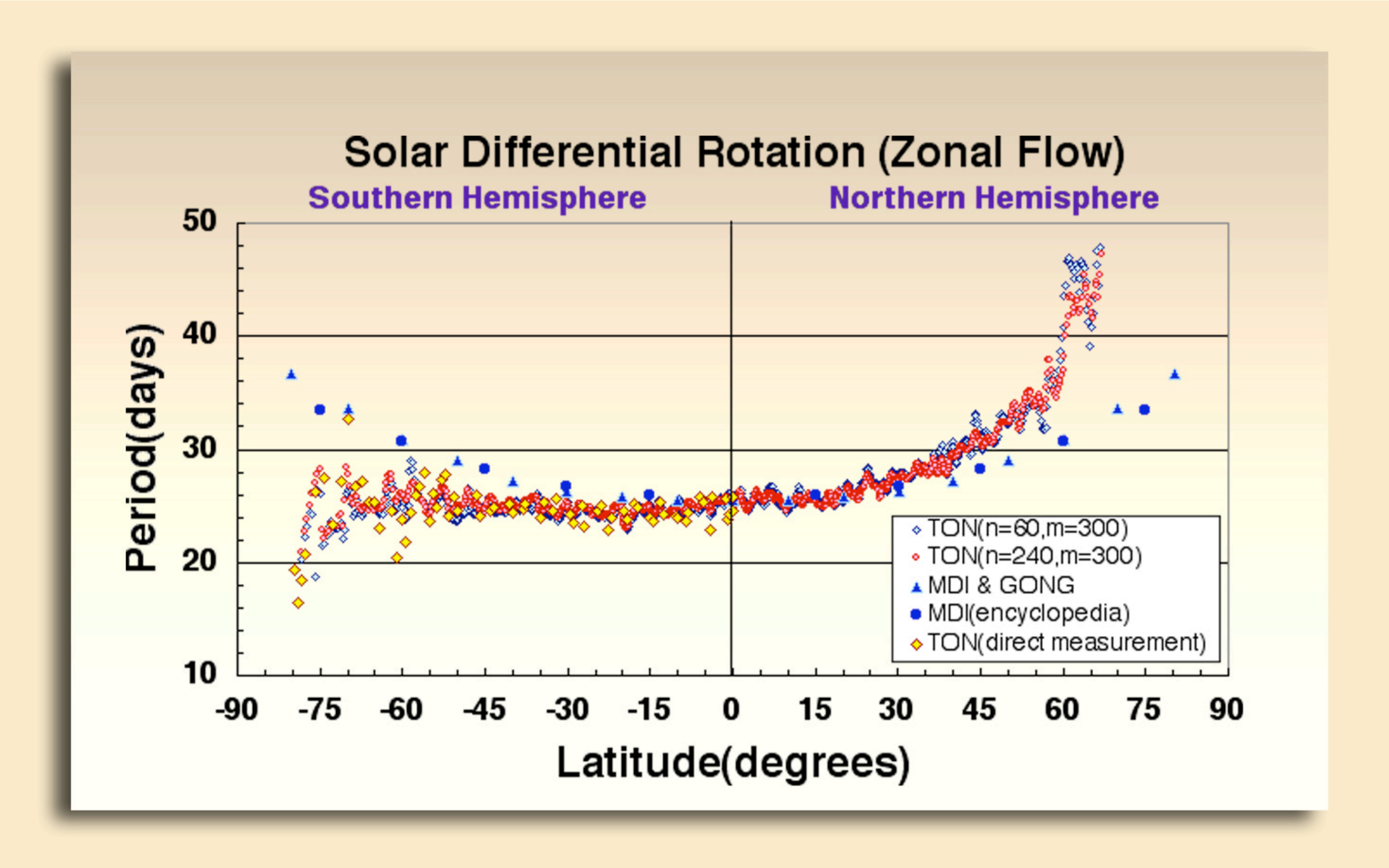

Solar Differential Rotation (Zonal Flow)
Southern Hemisphere
Northern Hemisphere
Period(days)
50
40
30
20
10
-90
-75
-60
-45
-30
-15
0
15
30
45
60
75
90
Latitude(degrees)
TON(n=60,m=300)
TON(n=240,m=300)
MDI & GONG
MDI(encyclopedia)
TON(direct measurement)